Characterization of three novel RNAi machinery components in *C. elegans*

By

Huan Yang

Submitted to the graduate degree program in Molecular and Integrative Physiology and the Graduate Faculty of the University of Kansas in partial fulfillment of the requirements for the degree of Doctor of Philosophy.

Chairperson Ho Yi Mak

Co-Chair Lane Christenson

Peter Baumann

Scott Hawley

Hao Zhu

Date Defended: March 25 2013

The Dissertation Committee for Huan Yang

certifies that this is the approved version of the following dissertation:

Characterization of three novel RNAi machinery components in *C. elegans*

Chairperson Ho Yi Mak

Co-Chair Lane Christenson

Date approved: April 11 2013

Abstract

RNA interference (RNAi) is a homology-based and antisense small RNA-dependent gene silencing mechanism found in most eukaryotes. This dissertation describes identification and characterization of three novel RNAi pathway components in nematode *Caenorhabditis elegans*: *rde-10*, *rde-11* and *rde-12*. We demonstrated that they are required for targeted mRNA degradation and the subsequent secondary siRNA biogenesis.

The molecular mechanisms for targeted mRNA degradation in *C. elegans* undergoing RNA interference (RNAi) are not fully understood. Using a combination of genetic, proteomic and biochemical approaches, we have identified a divergent RDE-10/RDE-11 complex that is required for RNAi in *C. elegans*. Genetic analysis indicates that the RDE-10/RDE-11 complex acts in parallel to nuclear RNAi. Association of the complex with target mRNA is dependent on RDE-1 but not RRF-1, suggesting that target mRNA recognition depends on primary but not secondary short interfering RNA (siRNA). Furthermore, RDE-11 is required for mRNA degradation subsequent to target engagement. Results of deep sequencing analyses reveal a 5-fold decrease in secondary siRNA abundance in *rde-10* and *rde-11* mutant animals, despite normal primary siRNA and micro-RNA biogenesis. Therefore, the RDE-10/RDE-11 complex is critical for amplifying the exogenous RNAi response. Our work uncovers an essential output of the RNAi pathway in *C. elegans*.

RDE-12, a putative DEAD-box RNA helicase, was identified from the same genetic screen. A GFP::RDE-12 fusion protein forms cytoplasmic foci in somatic cells and resides in peri-nuclear P granules in the germline. RDE-12 engages target mRNAs in response to RNAi and is required for the secondary siRNA biogenesis. We hypothesize that RDE-12 acts as a linkage between mRNA targeting and secondary siRNA synthesis in the RNAi pathway.

Acknowledgements

I want to express sincere appreciation to everyone who provided advice and help during my PhD training. A special thanks to my advisor, Ho Yi Mak, for discussions and help, and for teaching me everything that will benefit my career development.

I sincerely appreciate that members of my dissertation examination committees took time in evaluating my research projects and defense presentation.

Thanks also to my wife Yuefei, with whose support I was able to complete research projects with enthusiasm.

TABLE OF CONTENTS

LIST OF ABBREVIATIONS

Abbreviations	Full name
Ago	Argonaute
dsRNA	Double-stranded RNA
endo-siRNA	endogenous short interfering RNA
exo-siRNA	exogenous short interfering RNA
miRNA	micro-RNA
Rde	RNAi defective
RdRP	RNA dependent RNA polymerase
RISC	RNA induced silencing complex
RNAi	RNA interference
piRNA	Piwi-interacting RNA
siRNA	short interfering RNA

LIST OF FIGURES

LIST OF TABLES

Chapter 1

General introduction

Overview of RNA interference

Before the discovery of RNA interference, the antisense RNA technique was used to inhibit gene expression in a sequence-specific manner (Izant and Weintraub 1984; Fire *et al.* 1991). Due to inconsistency and marginal efficacy, this technique was considered unreliable. Especially, researchers found that sense RNA could also inhibit gene expression (Guo and Kemphues 1995). Later, researchers found that double stranded RNA (dsRNA), the byproduct of antisense RNA preparations, was the trigger of this dsRNA-mediated interference (Fire *et al.* 1998), which was eventually named RNA interference (RNAi). RNAi has been widely utilized at every aspect of biomedical research since it is capable of facilitating genetic analysis without genetic mutants. RNAi in *C elegans* can be easily induced by feeding bacteria that express dsRNA. The convenience of genetic manipulation and laboratory husbandry of *C. elegans* makes it an ideal model organism for studying the basic mechanism of RNAi.

Double-stranded RNA (dsRNA), when introduced into cells of eukaryotes, can cause degradation of mRNAs that contain sequences homologous to the trigger dsRNA. Eukaryotes employ proteins similar to those in worms, such as Dicer and Argonaute, to achieve gene silencing. The process of RNAi can generally be divided into three steps: dsRNA cleavage, RNA Induced Silencing Complex (RISC) assembly, and target mRNAs silencing (Fig 1.1) (Hammond *et al.* 2000; Elbashir *et al.* 2001; Ketting *et al.* 2001; Knight and Bass 2001). dsRNA is cleaved by RNase III Dicer-like protein into 21-25 nucleotide RNA duplexes (Elbashir *et al.* 2001; Ketting *et al.* 2001; Knight and Bass 2001). One strand of the duplex, termed siRNA, is selectively loaded into RISC (Martinez *et al.* 2002; Khvorova *et al.* 2003; Schwarz *et al.* 2003; Tomari *et al.* 2004).

RISC is the effector complex for gene silencing. Argonaute Family proteins, the key components of RISCs, directly bind siRNAs to recognize the target and to mediate gene silencing at transcriptional and post-transcriptional level (Tabara *et al.* 1999; Hammond *et al.* 2001; Liu *et al.* 2004; Batista *et al.* 2008; Guang *et al.* 2008; Claycomb *et al.* 2009; Gu *et al.* 2009; Buckley *et al.* 2012). One of the current major caveats in RNAi-based gene therapy is that essential small RNA regulatory pathways are impaired after introducing siRNA(Grimm *et al.* 2006). Therefore, further understanding about how distinct silencing mechanisms are employed by divergent RNAi pathway components will provide insights for RNAi-based gene therapy.

Dicer dices dsRNA

Dicer proteins act at the initial phase of RNAi to cut dsRNA into ~21-25 nt small RNA duplex (Bernstein *et al.* 2001; Ketting *et al.* 2001; Knight and Bass 2001). The Dicer family is evolutionarily conserved in worms, flies, plants, fungi and mammals. Humans and *C. elegans* only have one dicer which is shared between the siRNA pathway and the miRNA pathway. Dicer proteins possess a helicase domain, two RNase III motifs and one PAZ domain. The two RNase III domains coordinate to cut dsRNAs (Weinberg *et al.* 2011), which makes Dicer as a molecular ruler to cut dsRNA into exact 21-25 nt small RNA duplex in different organisms. PAZ domain, also observed in Argonaute proteins, has been shown to recognize dsRNA ends and specify siRNA length (Zhang *et al.* 2004; MacRae *et al.* 2007). In flies, R2D2 (the homolog of RDE-4 in *C. elegans*) bridges the initial step and the effector step of RNAi pathway by facilitating siRNA handover from Dicer to Argonaute proteins (Fig 1.1) (Liu *et al.* 2003; Tomari *et al.* 2004). This handover

process is also facilitated by heat shock protein chaperone machinery (Iwasaki *et al.* 2010; Miyoshi *et al.* 2010)

Distinct Argonautes for multiple silencing mechanisms

Argonaute proteins act in distinct pathways, such as developmental regulation (miRNA pathway) (Fig 1.2) (Grishok *et al.* 2001), genome integrity (Fig 1.3) (Batista *et al.* 2008; Gu *et al.* 2012), chromosome segregation (Fig 1.4) (Claycomb *et al.* 2009), exo-RNAi (Fig 1.1) (Tabara *et al.* 1999; Yigit *et al.* 2006; Guang *et al.* 2008; Buckley *et al.* 2012), and the newly defined endo-RNAi (Fig 1.4) (Gu *et al.* 2009; Conine *et al.* 2010; Vasale *et al.* 2010) . The *C. elegans* RDE-1 (RDE: RNAi defective) is the first Argonaute protein identified from the study of RNAi defective mutants. Later, mouse Ago2 (Hammond *et al.* 2001; Liu *et al.* 2004), an ortholog of RDE-1, was also shown to be essential for RNAi. Argonaute proteins dedicated to the RNAi pathway contain two conserved domains, PAZ and PIWI. Structural analyses show that PAZ domain holds the 3' end of siRNA (Song *et al.* 2004) while the MID-PIWI interface provides the binding pocket for the 5' end of siRNA (Boland *et al.* 2011). The PIWI domain in Argonaute proteins has a tertiary structure similar to that of RNase H. Several Argonaute proteins have been shown to slice target mRNAs in the middle of the siRNA binding site via RNase H-like activity *in vivo* and *in vitro* (Hammond *et al.* 2001; Liu *et al.* 2004; Meister *et al.* 2004; Aoki *et al.* 2007).

The *C. elegans* genome is predicted to encode 23 functional Argonaute proteins. Those dedicated to RNAi pathway can be divided into two groups, the primary Argonaute (RDE-1) and the secondary Argonautes (Fig 1.1) (Yigit *et al.* 2006). These secondary Argonautes, also known as worm-specific Argonautes (WAGO), are results of

unique Argonaute protein family expansion in nematode. RDE-1 binds primary siRNA that is directly generated from dsRNA trigger. RRF-1, an RNA dependent RNA polymerase, then can use the target mRNA as the template to synthesize antisense siRNA (Fig 1.1) (Sijen *et al.* 2001; Sijen *et al.* 2007). The siRNA generated through amplification by RRF-1 is called secondary siRNA and is loaded into WAGOs. WAGO loss of function mutants (Yigit *et al.* 2006), similar to the primary Argonaute mutant *rde-1*, confer an RNAi defective phenotype, which suggests that these WAGOs play an important role in RNAi (Fig 1.1). Surprisingly, WAGOs lack the key catalytic residues of RNase H which are required for the slicing activity (Yigit *et al.* 2006). Therefore, WAGOs are expected to cooperate with additional factors to mediate target mRNA turnover. One WAGO that was defined very recently is NRDE-3 (NRDE: Nuclear RNAi DEfective) (Guang *et al.* 2008). NRDE-3, together with NRDE-2 (a novel protein containing a conserved domain of unknown function 1740) (Guang *et al.* 2010), mediates targeted gene silencing by inhibiting transcription elongation. It is still unknown how other WAGOs mediate gene silencing, which may potentially be achieved through translational repression or target mRNA degradation.

The endogenous RNAi pathway employs naturally generated endogenous siRNA to regulate gene expression without the introduction of exogenous dsRNA triggers. In *C. elegans*, based on the length and 5' nucleotide of the endo-siRNAs and their interacting Argonaute proteins, endo-siRNA pathways are classified into ERGO-1 26G, ALG-3/4 26G, and CSR-1 22G pathways (Fig 1.4) (Claycomb *et al.* 2009; Gu *et al.* 2009; Han *et al.* 2009; Conine *et al.* 2010; Vasale *et al.* 2010). These pathways regulate genome integrity at both transcriptional and posttranscriptional level. Several components of exo-

RNAi have been shown to be required for the accumulation of a subpopulation of endo-siRNAs (Lee *et al.* 2006; Gent *et al.* 2010; Zhang *et al.* 2011). It is still not clear how these components of exo-RNAi pathway participate in the synthesis of some endo-siRNAs but not the others.

ERGO-1 26G small RNAs are endo-siRNAs enriched in oocytes and early embryos of *C. elegans* (Fig 1.4) (Han *et al.* 2009; Vasale *et al.* 2010). The molecular mechanism of ERGO-1 26G biogenesis is not clear, although several molecular requirements have been identified (Han *et al.* 2009; Vasale *et al.* 2010). Abolishment of the ERGO-1 pathway cause enhanced exo-RNAi effect and reduced brood size under high temperature in *C. elegans* (Han *et al.* 2009; Pavelec *et al.* 2009; Vasale *et al.* 2010). The function of ERGO-1 26G pathway is not clear, however, the targets of ERGO-1 26G RNA are not random and appear to undergo recent gene duplications.

ALG-3/4 26G small RNAs are endo-siRNAs enriched in sperms and targeting spermatogensis-enriched mRNAs which are eventually down-regulated by ALG-3/4 26G RNAs (Fig 1.4) (Conine *et al.* 2010). ALG-3/4 localizes to P granules which are considered to be a major site of posttranscriptional regulation in germline (Conine *et al.* 2010).

Both ERGO-1 26G and ALG-3/4 26G RNAs are Dicer-dependent primary siRNAs. Similar to primary siRNAs in the exo-RNAi pathway, primary endo-siRNAs can initiate secondary siRNAs synthesis. These secondary siRNAs, called WAGO 22G RNAs, are bound by a redundant set of worm specific Argonaute proteins (Fig 1.4) (Yigit *et al.* 2006; Gu *et al.* 2009; Vasale *et al.* 2010). The secondary siRNAs in both the exo-RNAi and the endo-RNAi pathways have strong propensity for a 5’ Guanosine (5’ G)

residue (Gu *et al.* 2009; Yang *et al.* 2012). It is still not clear what the molecular mechanism is, presumably because of the higher affinity between GC base pair than AT base pair. The WAGO 22G-RNA system silences transposons, pseudogenes, cryptic loci, as well as about 50% coding genes (Gu *et al.* 2009; Zhang *et al.* 2011). It is conceivable that almost every aspect of physiological functions is under the control of WAGO 22G. The external signal for the regulation of WAGO 22G RNAs system on gene expression is not clear either, although elevated temperature changes the pattern of WAGO 22G RNA(Vasale *et al.* 2010). It has been hypothesized that the WAGO 22G system confers the physiological robustness of animals to the variable environment (Gu *et al.* 2009).

RNA-dependent RNA polymerases (RdRPs)

In fungi, plants and *C. elegans*, RNA-dependent RNA polymerases (RdPPs) play an essential role in RNA mediated gene silencing. (Cogoni and Macino 1997; Mourrain *et al.* 2000; Catalanotto *et al.* 2002; Pak and Fire 2007; Sijen *et al.* 2007; Lee *et al.* 2010). In fungi and plants, RdRPs are recruited to aberrant RNAs or cleaved target mRNAs to synthesize the complementary strand, which results in dsRNA (Ghildiyal and Zamore 2009; Lee *et al.* 2010). These dsRNAs can then be cut into small RNA duplex by Dicer. In *C. elegans*, however, secondary siRNA biogenesis is Dicer in-dependent as shown by *in vivo* and *in vitro* results (Fig 1.1) (Aoki *et al.* 2007; Pak and Fire 2007; Sijen *et al.* 2007). There are four members of RdRP in *C. elegans*, EGO-1, RRF-1, RRF-2 and RRF-3 (Smardon *et al.* 2000). The function of RRF-2 is still unclear (Sijen *et al.* 2001), RRF-3 is required for ERGO-1 26G RNA biogenesis (Gent *et al.* 2009; Gu *et al.* 2009; Pavelec *et al.* 2009; Gent *et al.* 2010). EGO-1 is required for germline development and

synthesizing secondary siRNAs for both exo-siRNA and endo-siRNA pathways (Fig 1.1 and 1.4) (Smardon *et al.* 2000; Claycomb *et al.* 2009; Gu *et al.* 2009). EGO-1 is essential for CSR-1 22G RNA pathway which is required for proper chromosome segregation. Surprisingly, it is still not clear what is the primary siRNA for the CSR-1 22G RNA pathway. RRF-1 is the major RdRP in somatic tissues and uses target mRNAs as templates to synthesize antisense secondary siRNAs, which determines the distinct distribution of secondary siRNAs polarity (5'→3' on the antisense strand) (Sijen *et al.* 2001; Pak and Fire 2007; Sijen *et al.* 2007). The secondary siRNAs are more abundant near the trigger region (Pak and Fire 2007; Sijen *et al.* 2007; Yang *et al.* 2012). Since the interaction between RDE-1 and RRF-1 has not been identified, it is not clear what is the signal for RRF-1 recruitment, but it does not seem to be the cleaved target mRNA generated by the slicer activity of RDE-1 (Pak *et al.* 2012). Both *rrf-1* and *ego-1* are required for endo-siRNA biogenesis (Gu *et al.* 2009; Gent *et al.* 2010; Vasale *et al.* 2010). Sequential roles of RdRPs in endo-siRNA pathways have been proposed: *rrf-3* is required for primary endo-siRNA biogenesis while *rrf-1* and *ego-1* are required for secondary endo-siRNA biogenesis (Gent *et al.* 2010; Vasale *et al.* 2010). It is worth noting that even *rrf-1* and *ego-1* mainly function in the soma and germline respectively, redundancy has been observed both in the exo-RNAi and the endo-RNAi pathways (Gu *et al.* 2009; Pak *et al.* 2012).

RNA helicases

RNA helicases comprise a large protein family that is involved in virtually all aspects of RNA metabolism. Although RNA helicases possess highly conserved domains, different

enzymes catalyze a wide spectrum of biochemical activities, including RNA duplex unwinding, protein displacement from RNA and strand annealing (Jankowsky and Fairman 2007). From multiple genetic screens and RNAi-based screens, several RNA helicases are found to be required for RNAi and transgene silencing in *C. elegans* (Tijsterman *et al.* 2002; Duchaine *et al.* 2006) and other organisms (Wu-Scharf *et al.* 2000; Garcia *et al.* 2012). For example, DEAD-box RNA helicase MUT-14 is required to trigger gene silencing by short antisense RNAs. However, most of these studies focused on the genetic analysis of RNA helicase mutants. The progress to determine RNA substrates and interacting factors of RNA helicases in RNAi pathway seems still slow. Through mutational and structural analyses, enzymatic activities of helicase have been allocated to its motifs (Jankowsky and Fairman 2007). However, the results of *in vitro* biochemical analyses were hampered by the presence of residual catalytic activities. An extensive mutational analysis on the helicase domain with physiological expression level *in vivo* could provide more reliable interpretation on the function of different motifs in RNA helicases.

Connection between transgene silencing and RNAi

The Rde (RNAi defective) genes described in this study were identified from a pilot genetic screen for transgene desilencing mutants. Transgene silencing and RNAi have been shown to share many common factors (Fig 1.5) (Grishok *et al.* 2005; Kim *et al.* 2005). In *C. elegans*, high-copy transgenes are established by microinjection of DNA containing genes of interest into the gonadal syncytium. Through random recombination, injected DNAs can form transmittable extrachromosomal arrays. During the random

recombination, the integrity of the gene within the transgenic array may be disrupted. Aberrant RNAs could be utilized as the template to form dsRNAs which are substrates of the RNAi machinery (Kelly *et al.* 1997; Montgomery and Fire 1998; Luo and Chen 2007). Despite the triggers of initial silencing are different from RNAi, transgene silencing pathway eventually, if not completely, utilizes the RNAi machinery to silence transgenes (Fig 1.5).

Genetic screen for genes involved in RNAi

Many genetic screens have been performed to identify novel Rde genes. The results are fruitful but were not able to cover every aspect of RNAi. The simplest screen is to feed mutagenized worms with dsRNA triggers targeting essential genes, and those "escapers" are Rde mutants (Tabara *et al.* 1999). Rde mutants will be viable but not those RNAi-competent animals. One pitfall of this kind of screen is that many genes involved in uptake of dsRNA will also be considered as Rde genes (Winston *et al.* 2002). To eliminate these false positive hits, Rde mutants were further tested by direct injection of dsRNA which is considered as a more efficient strategy to induce RNAi. *rde-1* and *rde-4* (required for dsRNA cleavage) were identified from this kind of screen (Tabara *et al.* 1999). By performing secondary genetic screen, false positive hits were avoided. But Rde mutants with partial loss of RNAi functionality were also eliminated from further study.

Another approach of searching for genes required for RNAi is to screen for genes required for transgene silencing. Several groups have utilized transgene desilencing phenotype to study RNAi related genes (Grishok *et al.* 2005; Kim *et al.* 2005; Fischer *et al.* 2008). Those studies usually use strains expressing two transgenes, a marker and

another transgene producing RNAi triggers. The marker transgene gave an easily observable phenotype (for example: GFP). The other transgene produced transcripts that can form dsRNAs. This approach seems to be not sensitive enough to identify mutants with weak Rde phenotype, presumably due to highly expressed triggers.

Therefore, identification of novel components of RNAi machinery relies on a model with high sensitivity but without requirement of trigger delivery.

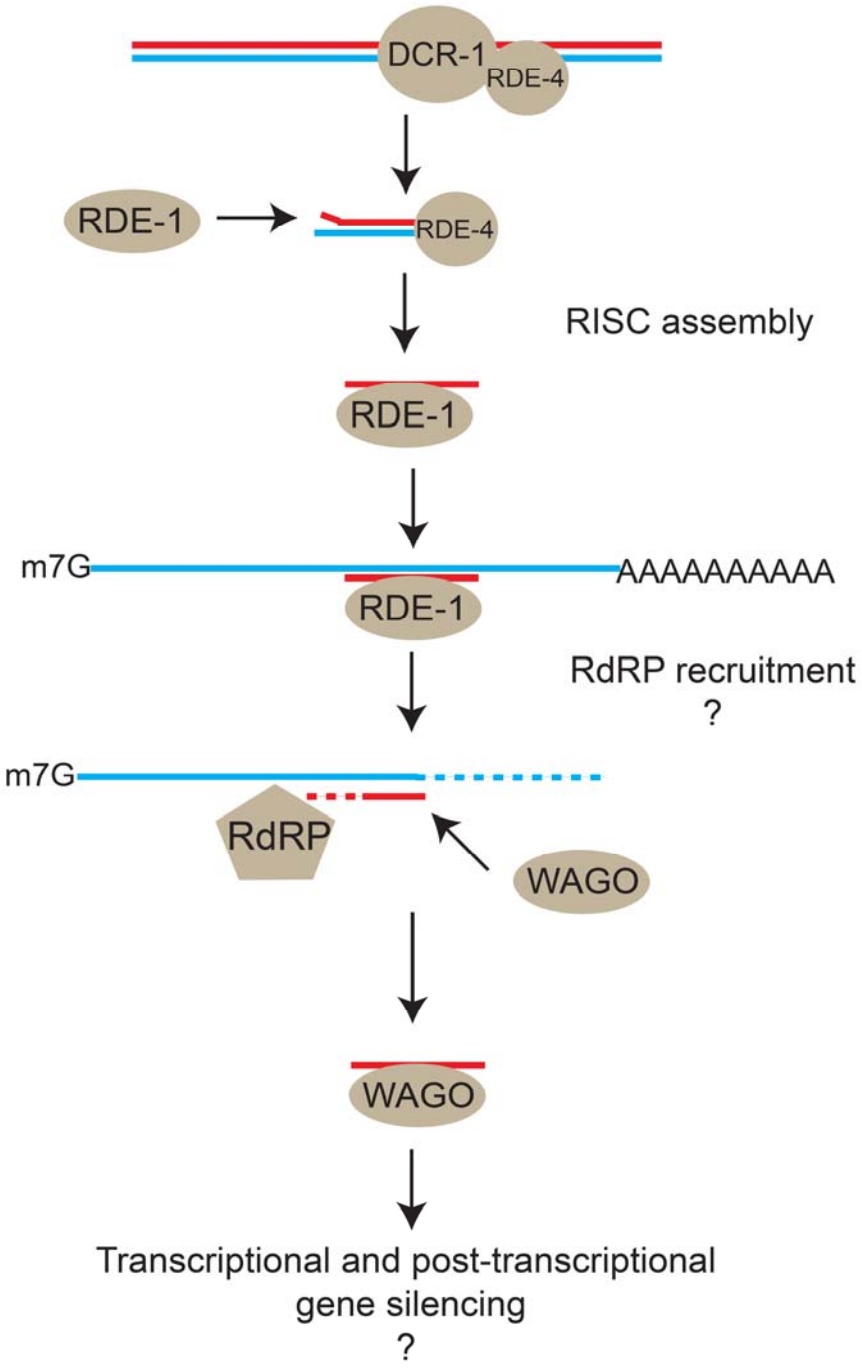

Figure 1.1. Exogenous RNAi pathway in *C. elegans*.

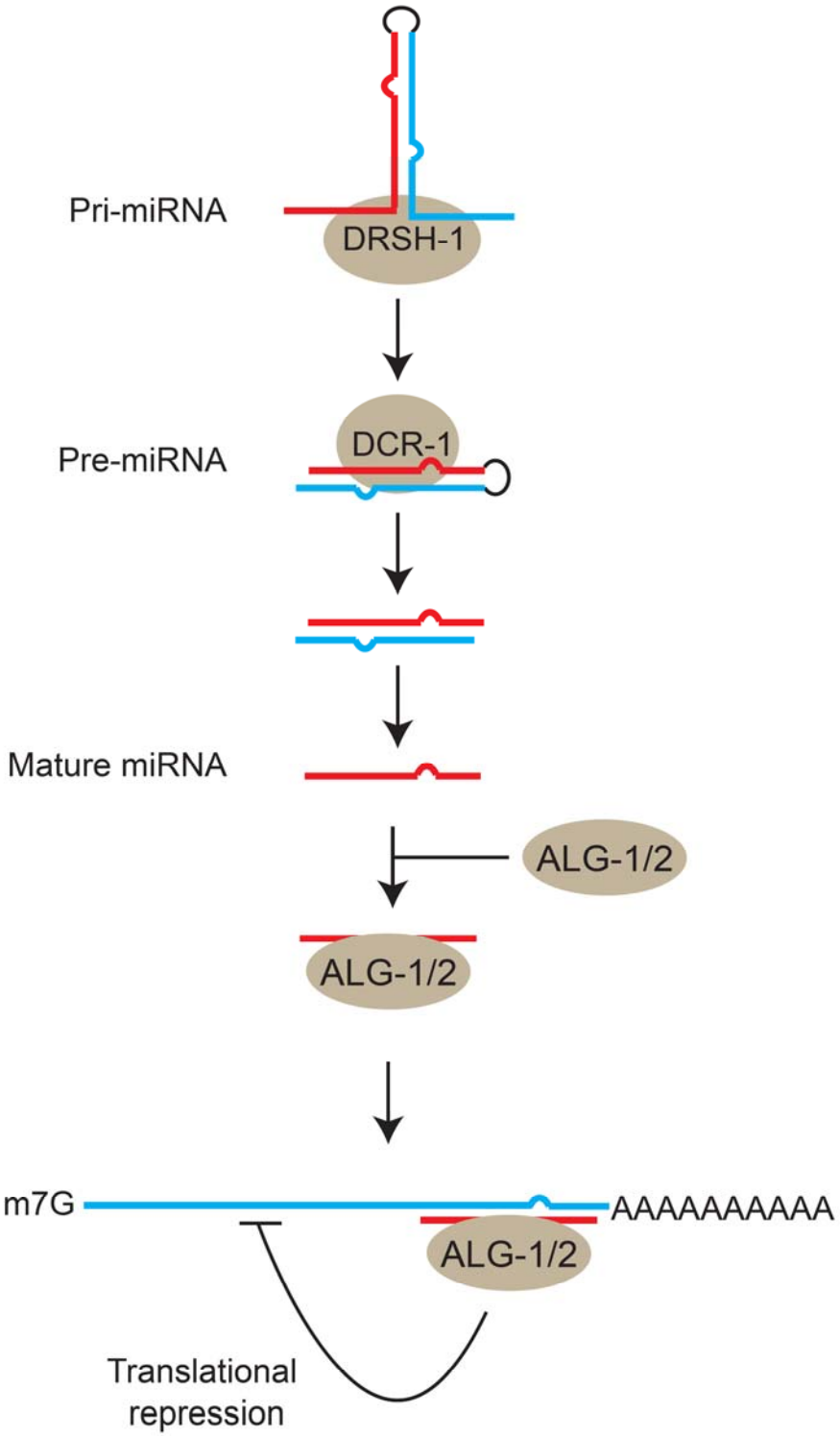

Figure 1.2. Micro-RNA pathway in *C. elegans*.

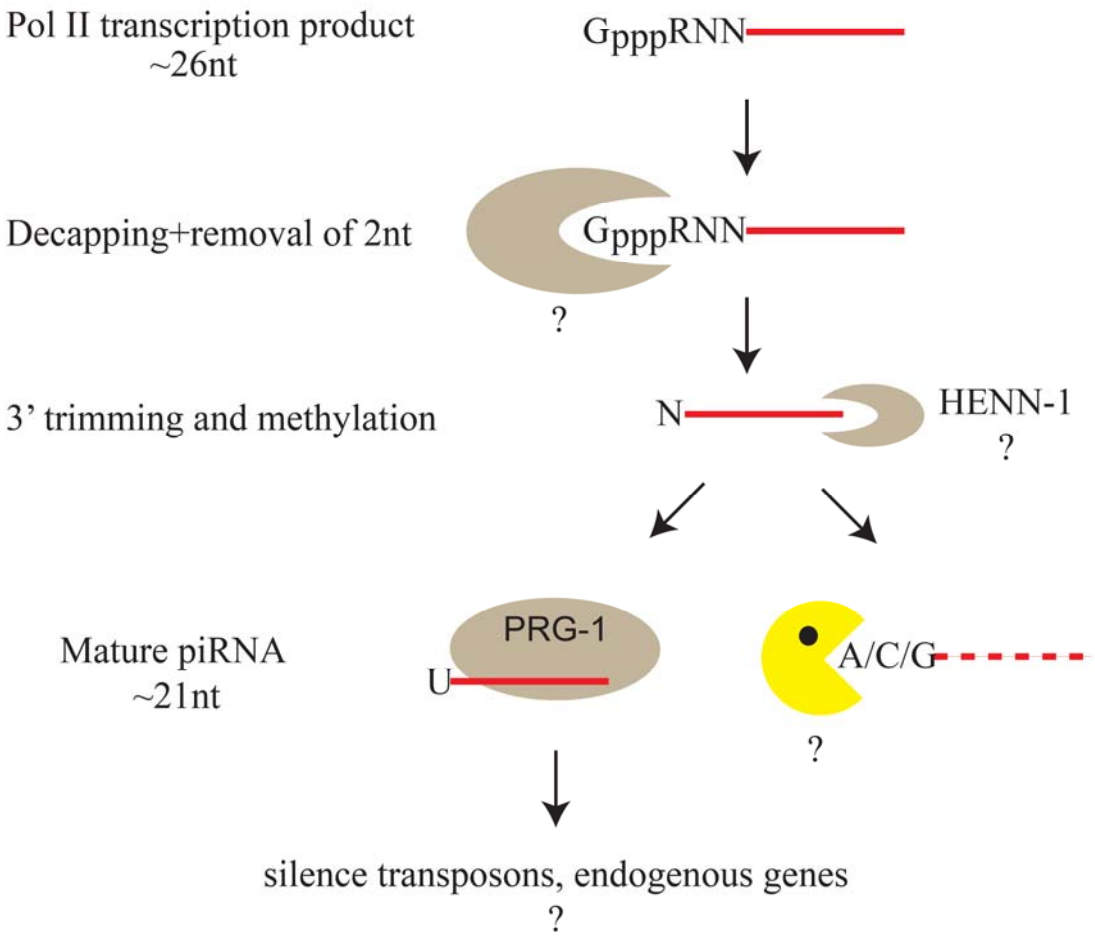

Figure 1.3. Simplified piRNA pathway in *C. elegans*. Adopted from (Gu *et al.* 2012)**.** The identities of several components are not discovered yet.

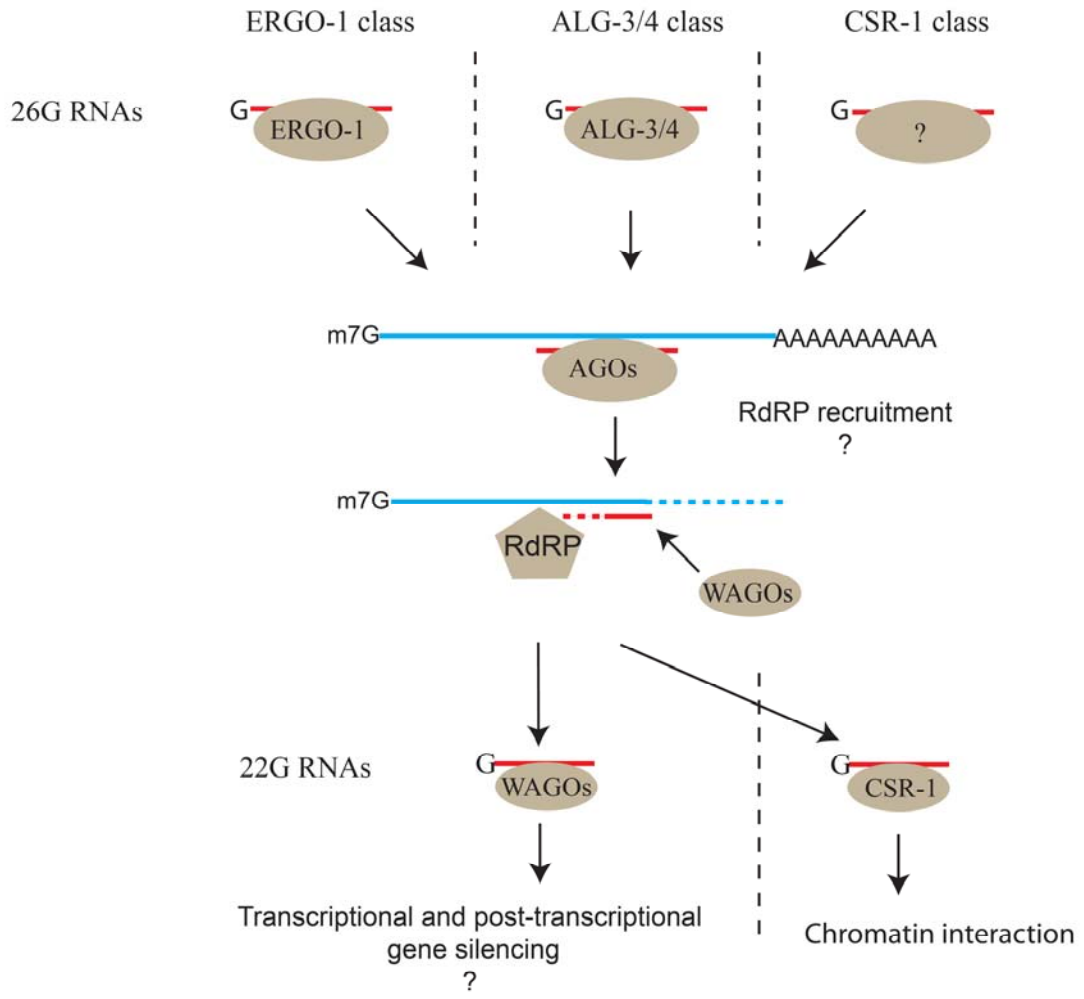

Figure 1.4. Endogenous RNAi pathway in *C. elegans*. ERGO-1 26G small RNAs are enriched in oocytes and early embryos**.** ALG-3/4 26G small RNAs are enriched in sperms. The triggers for CSR-1 22G small RNAs are not discovered yet.

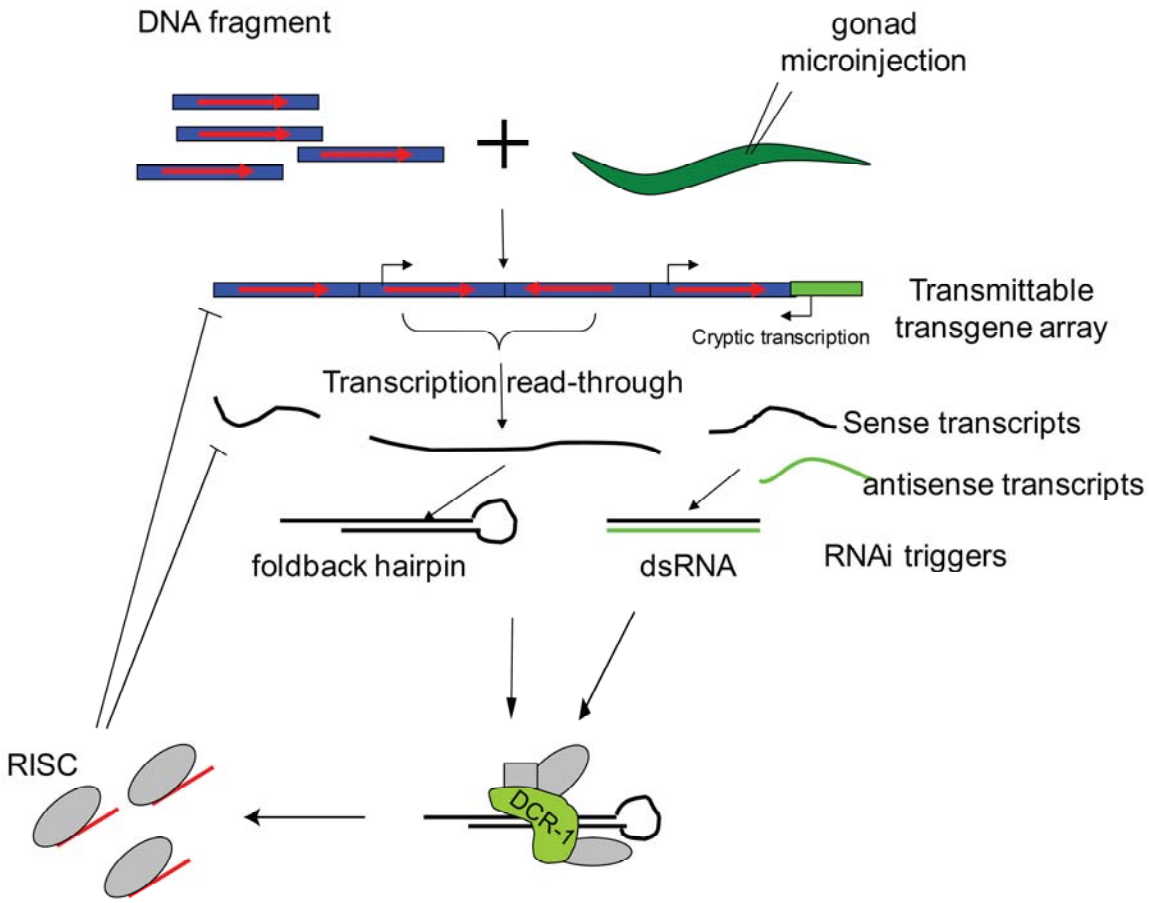

Figure 1.5. Transgene silencing shares similar molecular mechanism with RNAi.

Chapter 2

The RDE-10/RDE-11 complex triggers RNAi induced mRNA degradation by association with target mRNA in *C. elegans*

Abstract

The molecular mechanisms for target mRNA degradation in *C. elegans* undergoing RNA interference (RNAi) are not fully understood. Using a combination of genetic, proteomic and biochemical approaches, we report a divergent RDE-10/RDE-11 complex that is required for RNAi in *C. elegans*. Genetic analysis indicates that the RDE-10/RDE-11 complex acts in parallel of nuclear RNAi. Association of the complex with target mRNA is dependent on RDE-1 but not RRF-1, suggesting that target mRNA recognition depends on primary but not secondary siRNA. Furthermore, RDE-11 is required for mRNA degradation subsequent to target engagement. Deep sequencing reveals a 5-fold decrease in secondary siRNA abundance in *rde-10* and *rde-11* mutant animals, while primary siRNA and micro-RNA biogenesis is normal. Therefore, the RDE-10/RDE-11 complex is critical for amplifying the exogenous RNAi response. Our work uncovers an essential output of the RNAi pathway in *C. elegans*.

Results and discussion

rde-10 and *rde-11* are required for transgene silencing and RNAi in *C. elegans*

We established a transgene *(hjIs21)* in *C. elegans* that expressed an ATGL-1::GFP fusion protein under the control of the *vha-6* promoter. The *vha-6* promoter is active in intestinal cells from embryonic stage to adult (Oka *et al.* 2001). Interestingly, *hjIs21* is gradually silenced during larval development such that the ATGL-1::GFP fusion protein is visible in L1 but not L4 animals (Fig. 2.1A). We measured the mRNA transcript level from the *hjIs21* transgene by quantitative PCR and found that it was reduced by 5-fold in L4 animals (Fig. 2.1B). The *hjIs21* transgene undergoes a unique cycle of de-silencing and silencing in every generation. We reasoned that identification of genes that are required for silencing *hjIs21* may reveal novel regulators of transgene silencing. Therefore, we mutagenized animals carrying the *hjIs21* transgene with EMS and screened for mutant alleles that conferred ATGL-1::GFP expression in adult animals. From this screen, we recovered two new alleles of *rde-1*, which suggests that the RNA interference (RNAi) pathway is required for silencing the *hjIs21* transgene. Accordingly, mutant animals that carried the *rde-1(ne300)* reference allele could also increase the mRNA transcript level of the *hjIs21* transgene and restored ATGL-1::GFP expression in the larval L4 stage (Fig. 2.1A and B). Our results suggest that the canonical RNAi pathway is indeed involved in silencing *hjIs21* and trigger degradation of *atgl-1::gfp* mRNA. We also identified two novel genes: *rde-10* and *rde-11* from our genetic screen. The *hjIs21* mRNA levels in these two mutants were elevated in the L4 stage (Fig. 2.1A&B). In addition, *rde-10* and *rde-11* mutants failed to undergo RNAi by feeding *E. coli* that expressed double-stranded RNA targeting the endogenous *pos-1* and *nhr-23* genes (Fig. 2.1C and Table 2.1).

Molecular cloning revealed lesions of 3 recessive alleles of *rde-10* and 1 recessive allele of *rde-11* (Fig. 2.2A and 2.2B). The transgene silencing (Fig. 2.1A) and Rde phenotypes (Fig. 2.1C) of *rde-10* and *rde-11* mutant animals can be rescued by single copy transgenes expressing wild-type RDE-10 and RDE-11, respectively. Taken together, our results strongly suggest that *rde-10* and *rde-11* are two novel genes that are required for transgene silencing and RNAi in *C. elegans*.

The *rde-10* and *rde-11* genes do not have orthologs outside the *Caenorhabditis* genus. *rde-10* encodes a protein without any conserved domain, while *rde-11* encodes a protein with a RING-type zinc finger domain, based on sequence homology search by SMART (Letunic *et al.* 2009). The *rde-10* and *rde-11* mutants have no defect in fertility, no chromosome non-disjunction (Him) phenotype and no apparent defect in reproductive development, which suggests that *rde-10* and *rde-11* are unlikely to be required for miRNA and piRNA pathways. In *rde-10* mutant animals, we also detected NRDE-3::GFP in the nucleus (Fig. 2.3), suggesting that the nuclear RNAi pathway is intact.

rde-10 and *rde-11* act in parallel of the nuclear RNAi pathway

To address whether *rde-10* and *rde-11* are required for RNAi ubiquitously, we performed RNAi to silence genes that are expressed in different tissues. Surprisingly, *rde-10* and *rde-11* mutant animals show variable degree of RNAi resistance (Table 2.1). They are resistant to RNAi against *pos-1*, *nhr-23* and *unc-15* but are only partially resistant to RNAi against *unc-22* and *lir-1*, which caused a twitcher phenotype and larval lethality, respectively (Table 2.1). Incomplete RNAi resistance in *rde-10* and *rde-11* mutants was

not dependent on target tissues since *unc-15* and *unc-22* were both expressed in body wall muscles. We hypothesize that *rde-10* and *rde-11* act in parallel of additional RNAi effector pathways that contribute differentially toward gene silencing on a gene-specific or RNAi trigger-specific basis.

RNAi mediated gene silencing in *C. elegans* can occur both in the cytoplasm and the nucleus (Guang *et al.* 2008). It has been reported that *nrde-3* mutants are defective for nuclear RNAi but not cytoplasmic RNAi (Guang *et al.* 2008). Accordingly, *nrde-3* mutants are sensitive to *unc-22* RNAi (Table 2.1). However, *rde-10;nrde-3* and *rde-11;nrde-3* double mutants were resistant to *unc-22* RNAi while *rde-10; rde-11* double mutants remained partially sensitive to *unc-22* RNAi (Table 2.1). Our results suggest that *rde-10* and *rde-11* act in the same genetic pathway for cytoplasmic RNAi and in parallel of the nuclear RNAi pathway. Consistent with this notion, we found that *lir-1* RNAi caused lethality in *rde-10* and *rde-11* mutants, as a result of nuclear RNAi against the nuclear-localized *lir-1::lin-26* polysictronic RNA and a loss of *lin-26* function (Table 2.1).

To further clarify the relative contribution of *nrde* genes, *rde-10* and *rde-11* for RNAi, we quantitated the endogenous mRNA levels of *unc-15* in different genetic backgrounds after *unc-15* RNAi. Using the *unc-15* mRNA level in *rde-1(ne300)* mutant as a reference, we observed >90% reduction of *unc-15* mRNA in wild-type animals (Fig. 2.4A). However, in *rde-10* and *rde-11* mutants, the mRNA levels were ~19-fold higher than that in wild-type animals. This indicates that *rde-10* and *rde-11* are required for efficient silencing of endogenous targets by RNAi. We noted that the *nrde-3* mutant was still proficient in cytoplasmic RNAi, which caused a ~80% reduction of *unc-15* mRNA

after RNAi (Fig. 2.4A). The *rde-10;rde-11* double mutant had similar levels of residual *unc-15* mRNA after RNAi as *rde-10* and *rde-11* single mutants (Fig. 2.4A). In contrast, we observed significant additive effect of RNAi deficiency in the *rde-10;nrde-3* double mutants. As a result, the level of *unc-15* mRNA in the *rde-10;nrde-3* mutant is comparable to that in the *rde-1* mutant (Fig. 2.4A). This additive effect can be reversed by introducing a wild-type *nrde-3* transgene into the *rde-10;nrde-3* double mutant (Fig. 2.4A). Additional experiments using *unc-22* RNAi support the same conclusion, though the *unc-22* RNAi trigger seemed to induce nuclear RNAi more efficiently (Fig. 2.4B). Taken together, we conclude that *rde-10* and *rde-11* function in the same genetic pathway that acts in parallel of the nuclear RNAi pathway.

RDE-10 and RDE-11 form a novel protein complex

We used a proteomics approach to address whether RDE-10 interacts with previously characterized RNAi pathway components. Using a single copy transgenic strain that expressed a FLAG-epitope tagged RDE-10, we affinity purified RDE-10 from a worm population enriched with L4 stage animals, followed by Multi-dimensional Protein Identification Technology (MudPIT) analysis. Consistent with our genetic analysis, RDE-11 was identified as a major RDE-10 interacting protein (Fig. 2.5A). We also detected RSD-2, which is required for systemic RNAi (Tijsterman *et al.* 2004), and ERGO-1, which is required for biogenesis of some endogenous 26G siRNA (Gent *et al.* 2010; Vasale *et al.* 2010). Identification of these two proteins suggests that RDE-10 may be involved in both exogenous and endogenous RNAi pathways.

The physical association between RDE-10 and RDE-11 was further confirmed by co-immunoprecipitation assays. We found that FLAG-epitope tagged RDE-10 could efficiently bind to HA-epitope tagged RDE-11 in worm lysates (Fig. 2.5B, lane 4). To address whether RDE-10 can directly interact with RDE-11, we performed the same assay using *in vitro* translated proteins. In the absence of Zn^{2+}, we detected very weak but reproducible interaction between RDE-10 and RDE-11 (Fig. 2.5D, lane 5). However, incubation of RDE-10 and RDE-11 in a buffer with 50μM Zn^{2+} strongly enhanced their interaction *in vitro* (Fig. 2.5D, lane 7). Since RDE-11 possesses a RING-type Zinc finger domain, we speculate that RDE-11 requires zinc for proper folding and subsequent interaction with RDE-10. Indeed, the RING finger domain is required for RDE-11 function since mutation in a single conserved cysteine in the RING finger could reduce its interaction with RDE-10 *in vitro* (Fig. 2.5C and 5E, lane 7) and abolish the rescuing activity of an *rde-11* transgene *in vivo* (Fig. 2.1C, *hjEx12*) but not the protein stability (Fig. 2.2C). Our results indicate that RDE-10 directly interacts with RDE-11 in a zinc-dependent manner to form a stable complex.

The RDE-10/RDE-11 complex associates with target mRNAs that are undergoing degradation

To further test the hypothesis that RDE-10 and RDE-11 are required for cytoplasmic mRNA degradation, we asked if the RDE-10/RDE-11complex could associate with mRNAs targeted by RNAi. To this end, we generated rescuing single copy transgenes that expressed epitope-tagged RDE-10 or RDE-11 (Fig. 2.1C). We chose *elt-2* as the

target transcript for RNA co-immunoprecipitation (RNA-IP) assays (Fig. 2.6A). Animals were fed *E. coli* that expressed double-stranded RNA against *elt-2* or an unrelated gene, prior to immunoprecipitation of RDE-10 or RDE-11. Wild-type animals treated with *elt-2* RNAi showed an 80% reduction in *elt-2* mRNA level (Fig. 2.7A). Despite such low abundance of *elt-2* mRNA, we detected ~170-fold enrichment of RDE-11 binding *elt-2* mRNA (Fig. 2.7B). We also found that RDE-10 preferentially associated with *elt-2* mRNA in the presence or absence of RDE-11 (Fig. 2.7B). Similar observations were made when we used *dpy-28* as the target gene (Fig. 2.6B). These results indicate that RDE-10 can be recruited to target mRNAs independent of RDE-11 and suggest that RDE-11 is not required for target mRNA recognition. As *rde-11* mutant animals are RNAi defective (Fig. 2.7A), these results also indicate that the recruitment of RDE-10 alone to target mRNAs is not sufficient to trigger RNAi.

To test whether RDE-10 requires siRNA for target mRNA recognition, we also performed RDE-10 RNA-IP in *rde-1(-)* and *rrf-1(-)* animals. While *rde-1(-)* animals are completely defective in primary and secondary siRNA biogenesis (Tabara *et al.* 2002), *rrf-1(-)* animals are unable to generate secondary siRNA in somatic tissues (Sijen *et al.* 2001; Sijen *et al.* 2007). We found that RDE-10 failed to associate with target mRNAs in *rde-1(-)* animals (Fig. 2.7B, Fig. 2.6B). In contrast, the association of RDE-10 with *elt-2* target mRNAs appeared to increase in *rrf-1(-)* animals (Fig. 2.7B). Such enhancement was not universal, since the association of RDE-10 with two additional somatically expressed mRNA targets, *flr-1* (Take-Uchi *et al.* 1998) and *sel-1* (Pak and Fire 2007) was comparable in wild-type and *rrf-1(-)* animals (Fig. 2.7C). Taken together, our results indicate that RDE-10 depends on primary but not secondary siRNA to engage target

mRNAs and support a model that RDE-10, and by extension RDE-11, acts downstream of RDE-1 and upstream of RRF-1.

Next, we examined the integrity of target mRNAs that were associated with the RDE-10/RDE-11 complex. We performed quantitative PCR (qPCR) to measure the relative abundance of regions that are 5' or 3' to the RNAi trigger in RDE-10 associated *elt-2* mRNAs. Interestingly, we observed a 70% reduction in their 3' region in an RDE-11 dependent manner (Fig. 2.7D). Such preferential 3' depletion was specific to *elt-2* mRNA that associated with RDE-10 and was not apparent in total RNA samples (Fig. 2.7E). Similar results were also observed in animals undergoing RNAi against *dpy-28* (Fig. 2.6C and D). Since mature mRNAs possess a 5' cap and a 3' poly(A) tail, we next asked if these structures were preserved in RDE-10 target mRNAs. Capped mRNA is resistant to the Terminator 5'-3' exonuclease (TEX) unless pre-treated with the Tobacco Acid Pyrophosphatase (TAP). We found that mRNA transcripts of a house-keeping gene, *gpd-3,* and RDE-10 associated target *elt-2* mRNA could both be degraded by TEX only after TAP pre-treatment (Fig. 2.7F and Fig. 2.9). Therefore, our results suggest that RDE-10 associated target mRNAs are capped at the 5' end.

The instability of the 3' region of RDE-10 associated target mRNAs could be caused by deadenylation. To directly test this possibility, we repeated our RDE-10 RNA-IP, followed by reverse transcription of bound mRNAs using random hexamer or oligo(dT) primers. The former allowed detection of RNAs with or without a poly(A) tail while the latter allowed selective detection of poly(A) mRNAs. The relative abundance of RDE-10 associated *elt-2* mRNA was decrease by 40% when the oligo(dT) primer was used (Fig. 2.10A and B). This decrease was observed in wild-type but not in *rde-11*

mutant animals. Our results imply that the 3' end of RDE-10 associated target mRNAs undergoes deadenylation and degradation in an RDE-11 dependent manner. The retention of a 5' cap of such mRNAs may confer transient stability of a region 5' to the RNAi trigger, which can serve as a template for secondary siRNA synthesis.

RDE-10 and RDE-11 are required for secondary siRNA biogenesis

Our analysis so far placed the RDE-10/RDE-11 complex at a step between RDE-1 and RRF-1 in the exogenous RNAi pathway in *C. elegans*. It is conceivable that the RDE-10/RDE-11 complex is required for amplification of the RNAi response. To test this hypothesis, we subjected wild-type, *rde-10* and *rde-11* mutant animals to RNAi against a somatic gene, *sel-1*, using a well-characterized trigger (Fig. 2.8A) (Pak and Fire 2007). We then purified small RNAs (21 to 24 nucleotides) from duplicate populations of animals and sequenced them using the Illumina platform. Each biological sample yielded on average 11 million reads. The abundance of primary siRNAs was comparable in wild-type, *rde-10* and *rde-11* mutant animals (Fig. 2.8B, Table 2.2). In contrast, a 5-fold decrease in secondary siRNAs was observed in *rde-10* and *rde-11* mutant animals (Fig. 2.8C, Table 2.2). A detailed small RNA profiling revealed that 22G RNAs are the major secondary siRNA and reduced in *rde-10* and *rde-11* mutants (Fig. 2.11). It is conceivable that the residual secondary siRNAs can be loaded to secondary Argonautes (WAGOs) to sustain low level of cytoplasmic and nuclear RNAi. Unlike the clear deficit in secondary siRNAs, we detected comparable levels of miRNAs (*let-7*, *mir-1* and *mir-66*) (Reinhart *et al.* 2000; Lau *et al.* 2001; Lee and Ambros 2001) and a piRNA (21UR-1) (Ruby *et al.*

2006; Batista *et al.* 2008) in wild-type, *rde-10* and *rde-11* mutant animals (Fig. 2.8D and 5E). In addition, the levels of endogenous siRNAs complementary to F37D6.3 (WAGO-1 target, (Gu *et al.* 2009)), E01G4.5 (NRDE-3 target, (Guang *et al.* 2008)) and *hcp-1* (CSR-1 target, (Claycomb *et al.* 2009)) were unchanged (Fig. 2.8E). Taken together, our results strongly suggest that the RDE-10/RDE-11 complex is required for secondary siRNA synthesis, which is critical for amplifying the exogenous RNAi response (Fig 2.12).

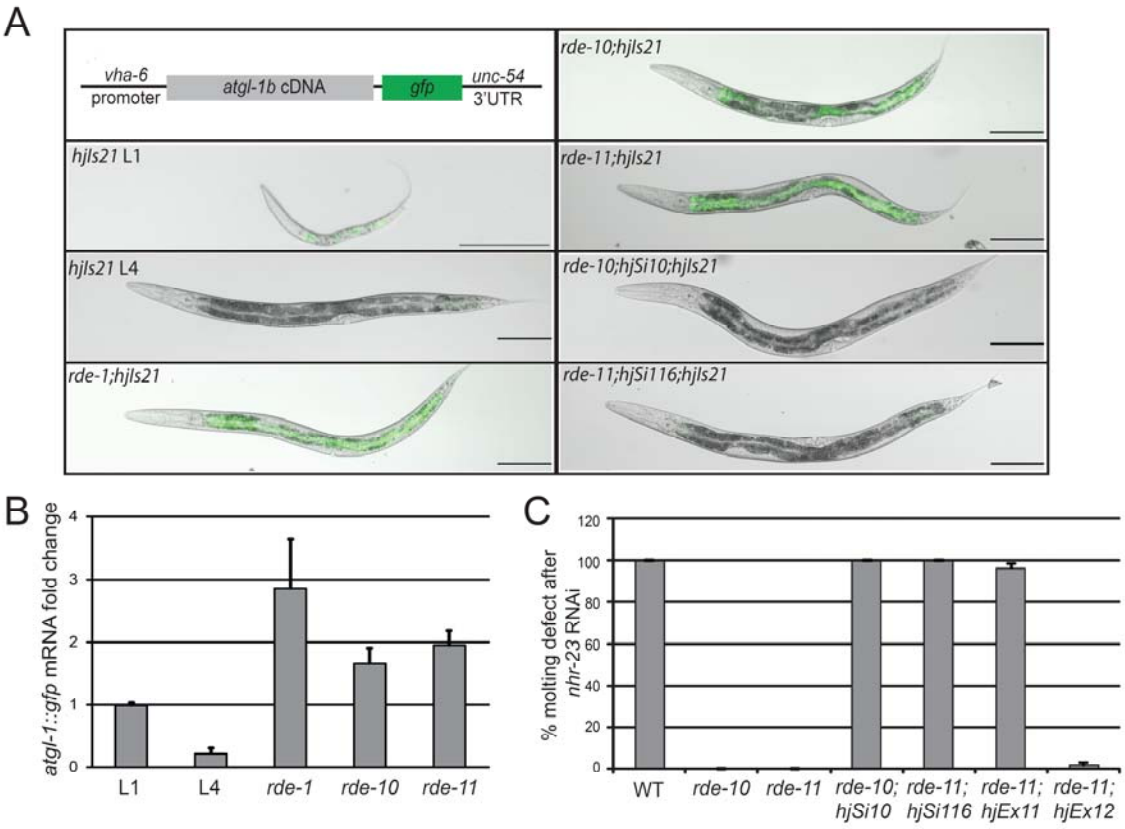

Figure 2.1. *rde-10* and *rde-11* are required for RNAi and transgene silencing. (A) Schematic representation of the *vha-6p::atgl-1b::gfp* transgene (*hjIs21*). Images of larval stage L1 or L4 wild-type animals carrying *hjIs21* are shown, together with *rde-1(ne300)*, *rde-10(hj20)*, *rde-11(hj37)*, *rde-10(hj20);hjSi10[rde-10(+)] and rde-11(hj37);hjSi116[rde-11(+)]* L4 mutant animals carrying the same transgene. Scale bar, 100μm. (B) Quantitation of *atgl-1::gfp* mRNA level by real-time PCR. The mRNA level in wild-type L1 animals was set as 1. Mean + standard deviation from triplicate reactions are shown. (C) Molting defect after *nhr-23* RNAi in wild-type, *rde-10(hj20)*, *rde-11(hj37)*, *rde-10(hj20); hjSi10[rde-10(+)]*, *rde-11(hj37); hjSi116[rde-11(+)]*, *rde-11(hj37);hjEx11[rde-11(+)] and rde-11(hj37);hjEx12[rde-11(C203S)]*. Mean + standard deviation from three independent experiments are shown.

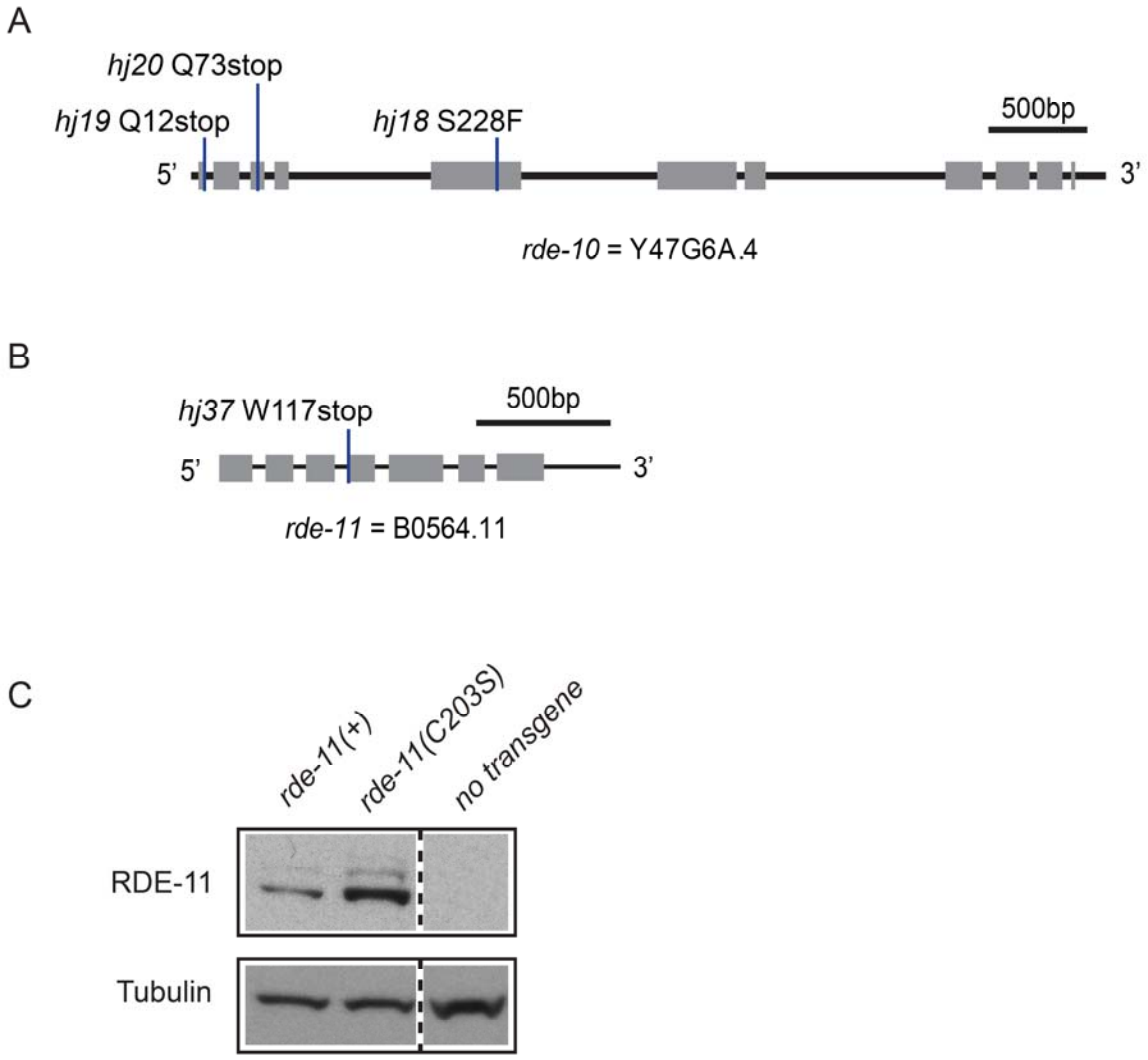

Figure 2.2. Gene structures of *rde-10* and *rde-11*. Exons are depicted in grey boxes. Mutant alleles and corresponding changes in protein coding sequences are indicated. (A) *rde-10*. (B) *rde-11*. (C) RDE-11 transgenes *hjEx11[rde-11(+)]* and *hjEx12[rde-11(C203S)]* expression levels. 100 transgenic animals were used for western blot.

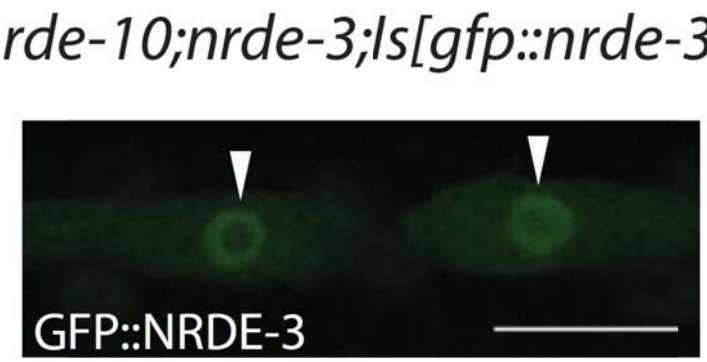

Figure 2.3. Localization of GFP::NRDE-3 fusion protein in *rde-10* mutant. Nuclear localization of GFP::NRDE-3 fusion protein in an *rde-10(hj20); nrde-3(gg66); ggIs1[nrde-3p::3xFLAG::GFP::nrde-3(+)]* L4 animal.

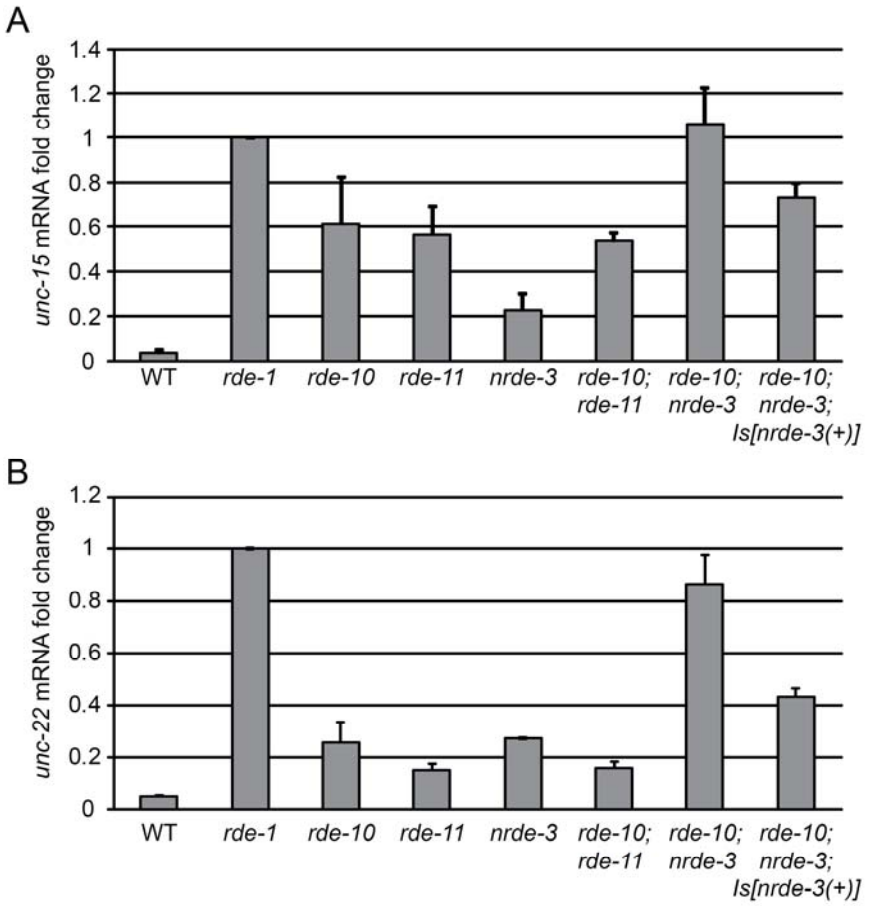

Figure 2.4. *rde-10* and *rde-11* act in parallel of the nuclear RNAi pathway to silence target genes. (A) Quantitation of endogenous *unc-15* mRNA levels after RNAi in wild-type (WT), *rde-1(ne300)*, *rde-10(hj20)*, *rde-11(hj37)*, *nrde-3(gg66)*, *rde-10(hj20)*; *rde-11(hj37)*, *rde-10(hj20); nrde-3(gg66)*, and *rde-10(hj20); nrde-3(gg66); Is[nrde-3(+)]* animals. The mRNA level in *rde-1* animals was set as 1. Mean + standard deviation from three independent samples assayed in triplicates are shown. (B) Quantitation of endogenous *unc-22* mRNA levels after RNAi in wild-type and mutant animals as in (A). Data are presented as in (A).

Figure 2.5. RDE-10 directly interacts with RDE-11 to form a stable complex. (A) MudPIT analysis on proteins co-immunoprecipitated with FLAG-tagged GFP::RDE-10 or GFP from worm extracts. dNASF (distributed normalized spectral abundance factors) indicates the relative abundance of proteins. Results are mean from 2 independent biological samples for GFP::RDE-10 and 3 independent biological samples for GFP. (B) Co-immunoprecipitation of HA-tagged RDE-11 with FLAG-tagged GFP::RDE-10 but not FLAG-tagged GFP from worm lysates. (C) Schematic representation of RDE-11. The RING-type Zinc finger is shaded in light grey and the zinc coordinating Cys and His residues are enlarged. Cys203 is boxed. (D) Co-immunoprecipitation of *in vitro* translated HA-tagged RDE-11 with FLAG-tagged RDE-10 in the presence or absence of Zn^{2+}. Direct interaction between RDE-10 and RDE-11 was strongly enhanced by Zn^{2+}. (E) Co-immunoprecipitation of *in vitro* translated wild-type and mutant HA-tagged RDE-11 with FLAG-tagged RDE-10 in the presence of Zn^{2+}. Interaction between RDE-10 and RDE-11 was impaired by the C203S mutation in the RING finger domain.

A

Name	Conserved domain	Phenotype	mean dNSAF	
			GFP::RDE-10 purification	GFP purification
GFP::RDE-10			0.03286	
GFP				0.09328
RDE-11	RING-type Zinc finger	Rde	0.00830	0.00000
ERGO-1	Argonaute	Eri	0.00095	0.00002
RSD-2	RSD-2 N-terminal domain	Rde	0.00051	0.00000

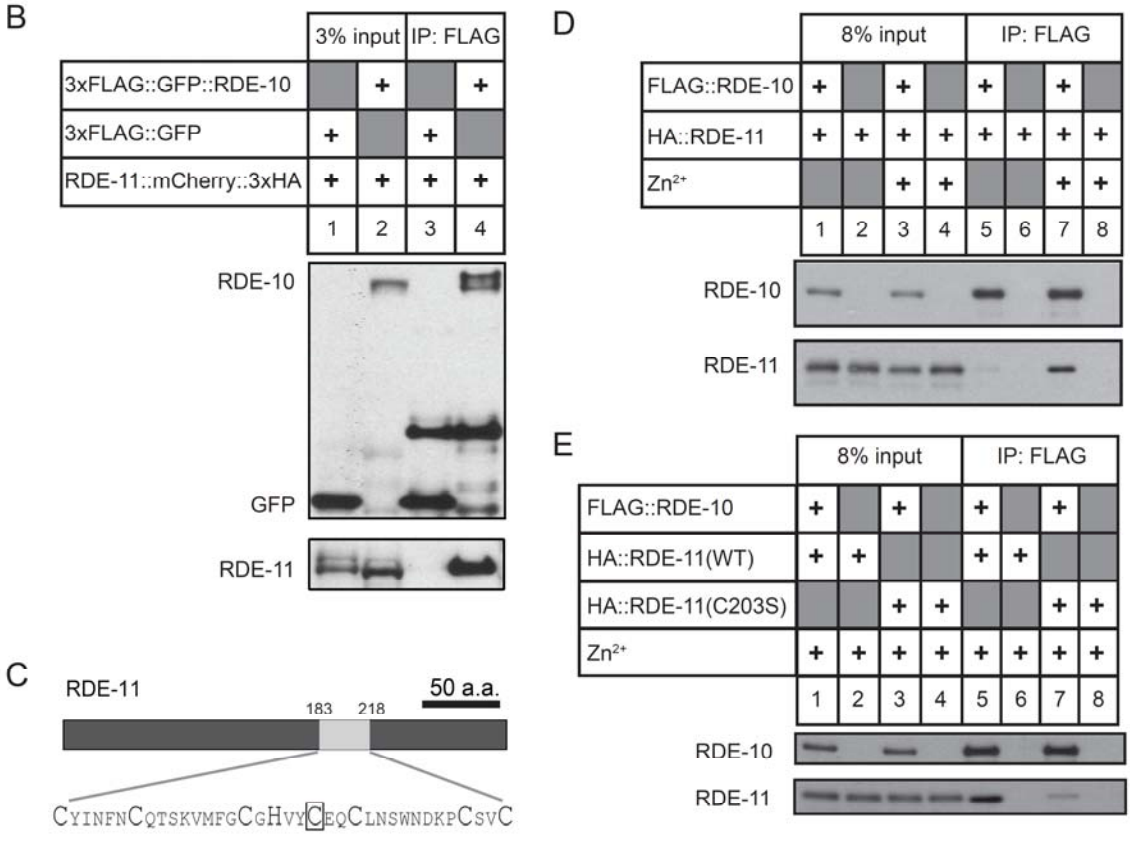

Figure 2.5. RDE-10 directly interacts with RDE-11 to form a stable complex.

Figure 2.6. The RDE-10/RDE-11 complex associates with *dpy-28* mRNA targeted by RNAi. (A) Experimental scheme for RNA co-immunoprecipitation (RNA IP) assays. (B) Target mRNA preferentially associated with RDE-10 in wild-type (WT), *rde-11(hj37)*, *rrf-1(pk1417)* but not *rde-1(ne300)* animals as shown by real-time PCR. Preferential association of target mRNA to RDE-11 was also observed in wild-type animals. The levels of *dpy-28* mRNA 5' to the RNAi trigger were measured. (C) Depletion of 3' end of target mRNA associated with RDE-10 in wild-type but not *rde-11(hj37)* animals. The levels of *dpy-28* mRNA 5' to the RNAi trigger were set as 1. (D) Comparison of relative abundance of *dpy-28* mRNA 5' and 3' to the RNAi trigger. Total RNA extracted from wild-type or *rde-11(hj37)* animals undergoing *dpy-28* RNAi was used. All results are shown as mean + standard deviation from at least three independent samples assayed in triplicates.

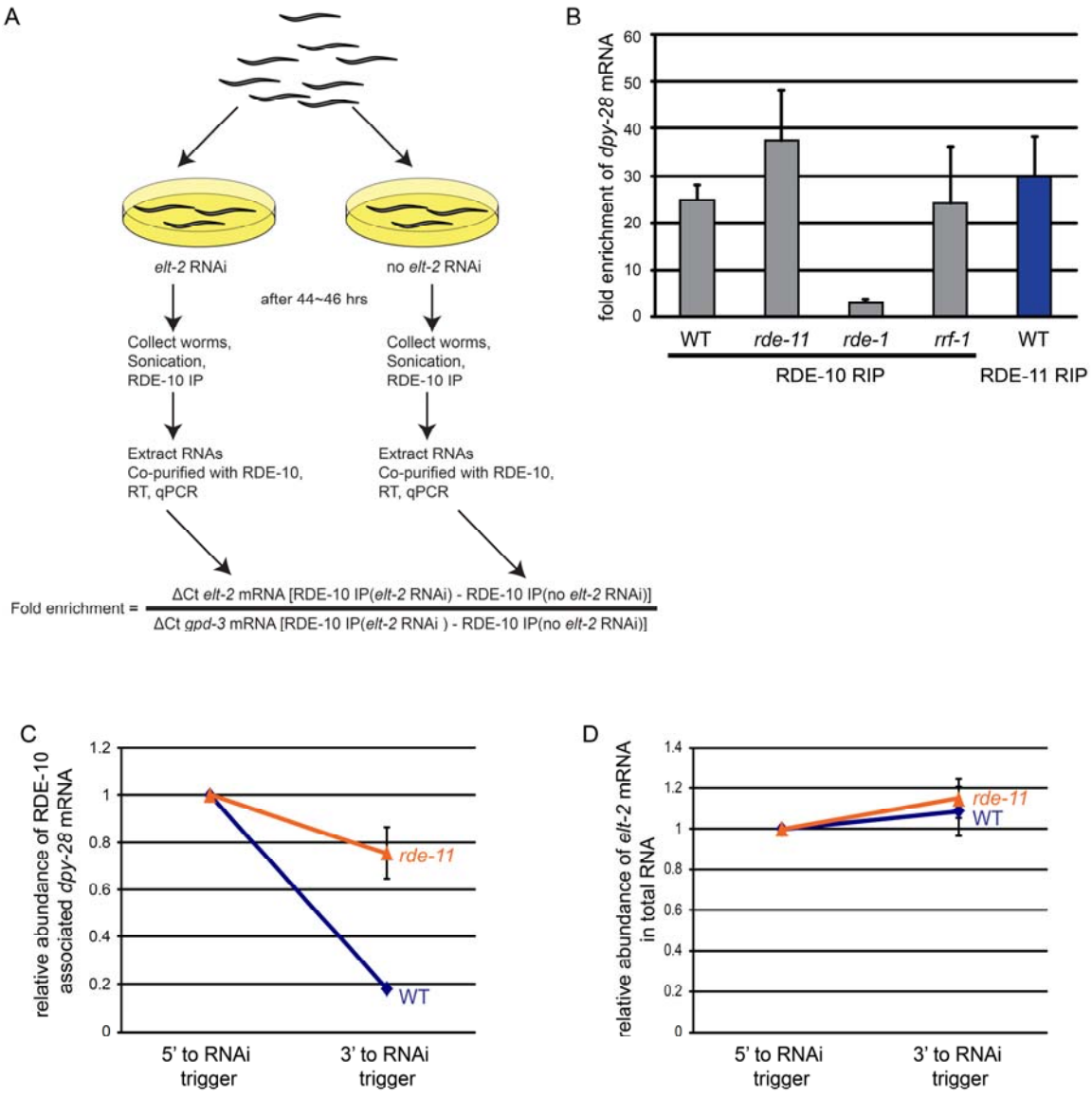

Figure 2.6. The RDE-10/RDE-11 complex associates with *dpy-28* mRNA targeted by RNAi.

Figure 2.7. The RDE-10/RDE-11 complex associates with mRNA targeted by RNAi. (A) Quantitation of *elt-2* mRNA levels by real-time PCR in wild-type (WT), *rde-11(hj37) rde-1(ne300)* or *rrf-1(pk1417)* animals undergoing *elt-2* RNAi. Each strain also carried *rde-10(hj20)* and the rescuing single copy transgene *hjSi10[rde-10(+)]*. The mRNA levels of *elt-2* in animals without RNAi treatment were set as 1 for each genotype. (B) Target mRNA preferentially associated with RDE-10 in wild-type (WT), *rde-11(hj37)*, *rrf-1(pk1417)* but not *rde-1(ne300)* animals as shown by real-time PCR. Preferential association of target mRNA to RDE-11 was also observed in wild-type animals. The levels of *elt-2* mRNA 5' to the RNAi trigger were measured. The formula for calculating fold-enrichment is shown. (C) Wild-type (WT) and *rrf-1(pk1417)* animals carrying *hjSi10* were subject to *flr-1* and *sel-1* RNAi. Target mRNAs, but not the non-specific *dpy-28* mRNA, preferentially associated with RDE-10 in wild-type and *rrf-1*animals. (D) Depletion of 3' end of target mRNA associated with RDE-10 in wild-type but not *rde-11(hj37)* animals. The levels of *elt-2* mRNA 5' to the RNAi trigger were set as 1. (E) Comparison of relative abundance of *elt-2* mRNA 5' and 3' to the RNAi trigger. Total RNA extracted from wild-type or *rde-11(hj37)* animals undergoing *elt-2* RNAi was used. (F) RDE-10 associated *elt-2* mRNA was resistant to TEX unless pre-treated with TAP. RNA samples were subject to Tobacco Acid Pyrophosphatase (TAP) and/or Terminator 5'-3' Exonuclease (TEX) treatments and were converted to cDNA and quantified with qPCR. The abundance of *elt-2* mRNA (RNAi target) in the sample without any treatment was set to 1. All results are shown as mean + standard deviation from at least three independent samples assayed in triplicates.

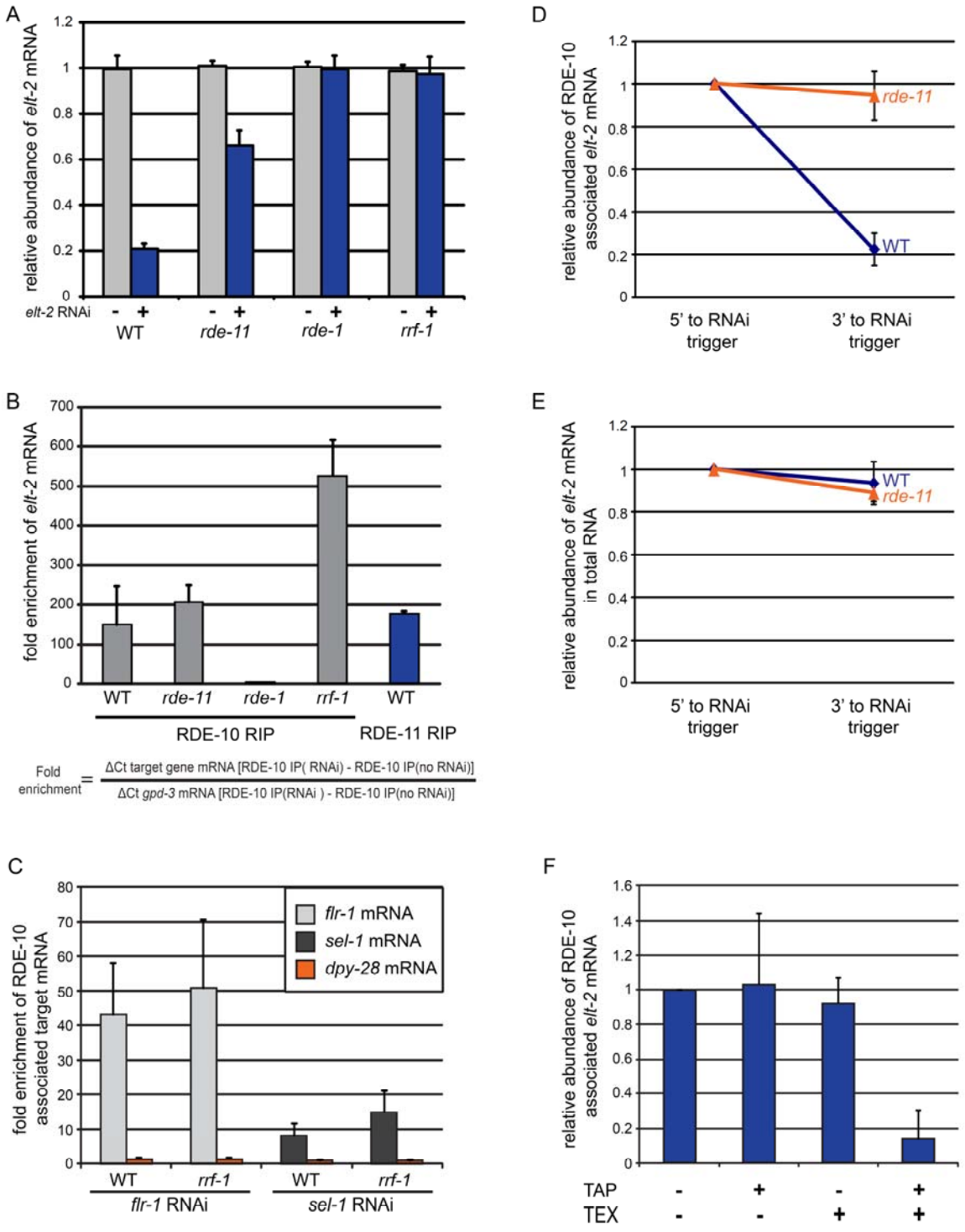

Figure 2.7. The RDE-10/RDE-11 complex associates with mRNA targeted by RNAi.

Figure 2.8. RDE-10 and RDE-11 are required for secondary siRNA synthesis. (A) Schematic representation of *sel-1* RNAi trigger and *sel-1* mRNA. (B-E) The mean abundance of small RNAs from two independent populations of wild-type, *rde-10(hj20)* and *rde-11(hj37)* animals undergoing *sel-1* RNAi is shown. (B) Sense *sel-1* siRNAs without TAP treatment. (C) Antisense *sel-1* siRNAs with TAP treatment. (D) Selected microRNAs (*mir*). (E) Selected endogenous siRNAs and one 21U-RNA. RPMs were calculated by (reads_aligned_to_region / all_aligned_reads_for_sample) * 1000000. A 5'-ligation-dependent method was used in library preparations. Small RNAs with 5' monophosphate were better represented in libraries without TAP treatment. Small RNAs with 5' triphosphate were better represented in libraries with TAP treatment.

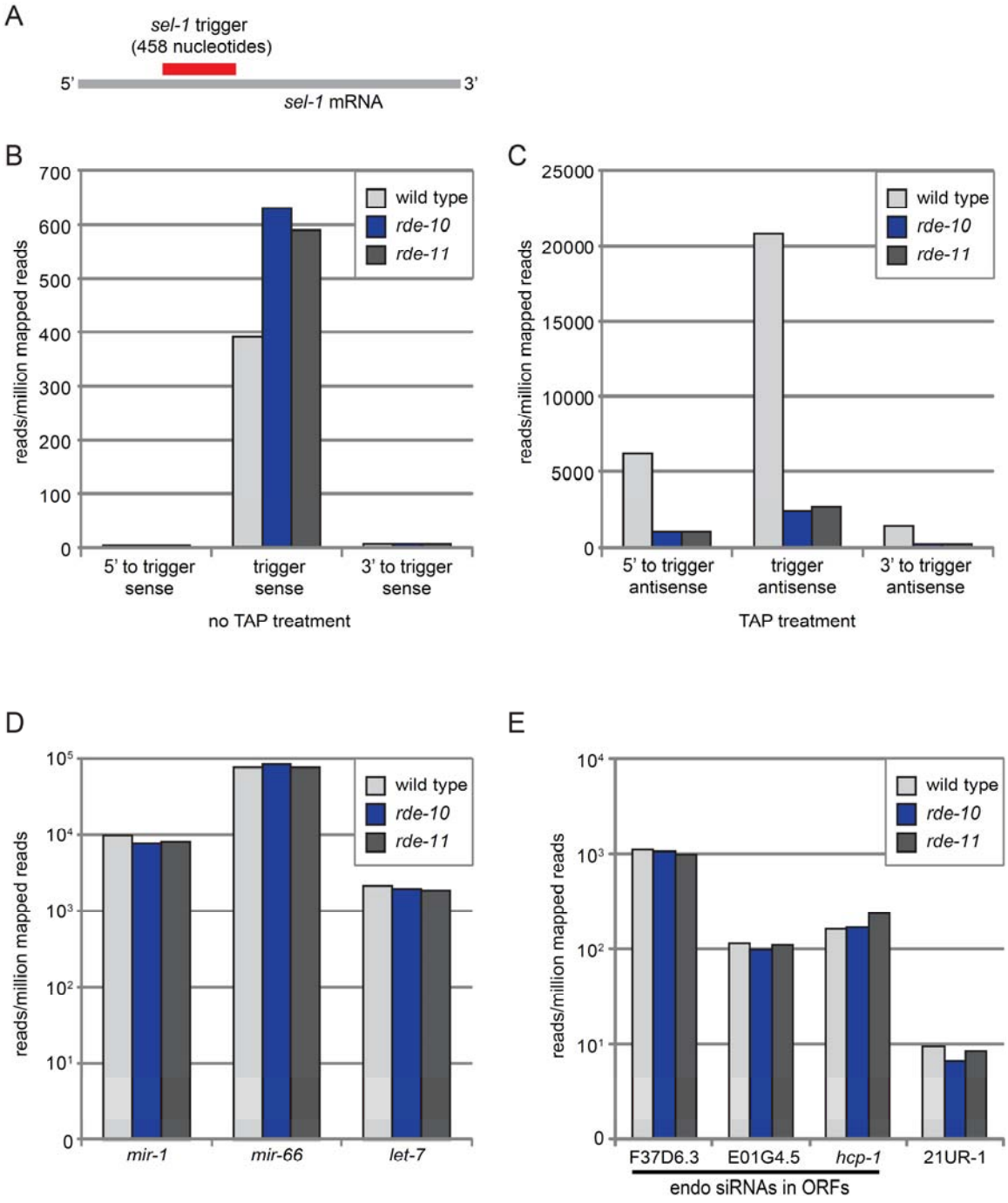

Figure 2.8. RDE-10 and RDE-11 are required for secondary siRNA synthesis.

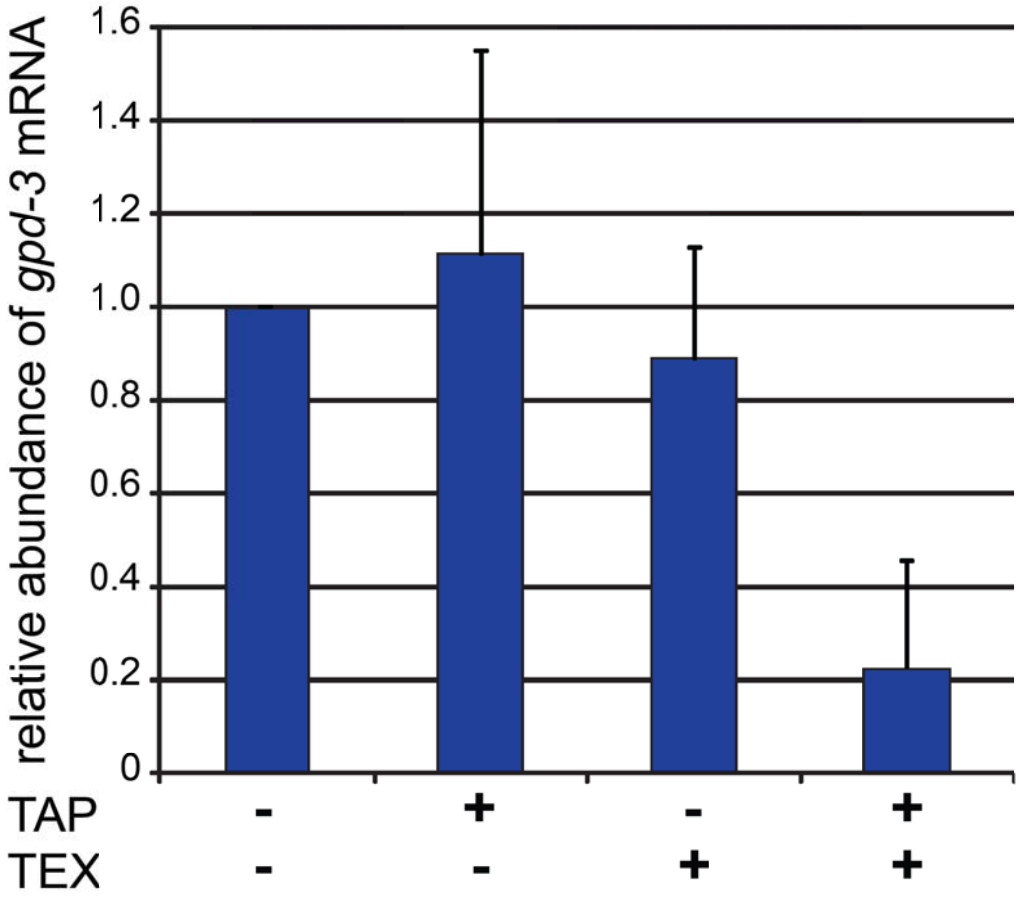

Figure 2.9. The *gpd-3* mRNA is 5' capped. The *gpd-3* mRNAs that associated with RDE-10 non-specifically in RNA-IP assays were subject to Tobacco Acid Pyrophosphatase (TAP) and/or Terminator 5'-3' Exonuclease (TEX) treatments. RNAs were converted to cDNA and quantified with qPCR. The abundance of *gpd-3* mRNA in the sample without any treatment was set as 1. The *gpd-3* mRNA was resistant to TEX unless pre-treated with TAP. All results are shown as mean + standard deviation from at least three independent samples assayed in triplicates.

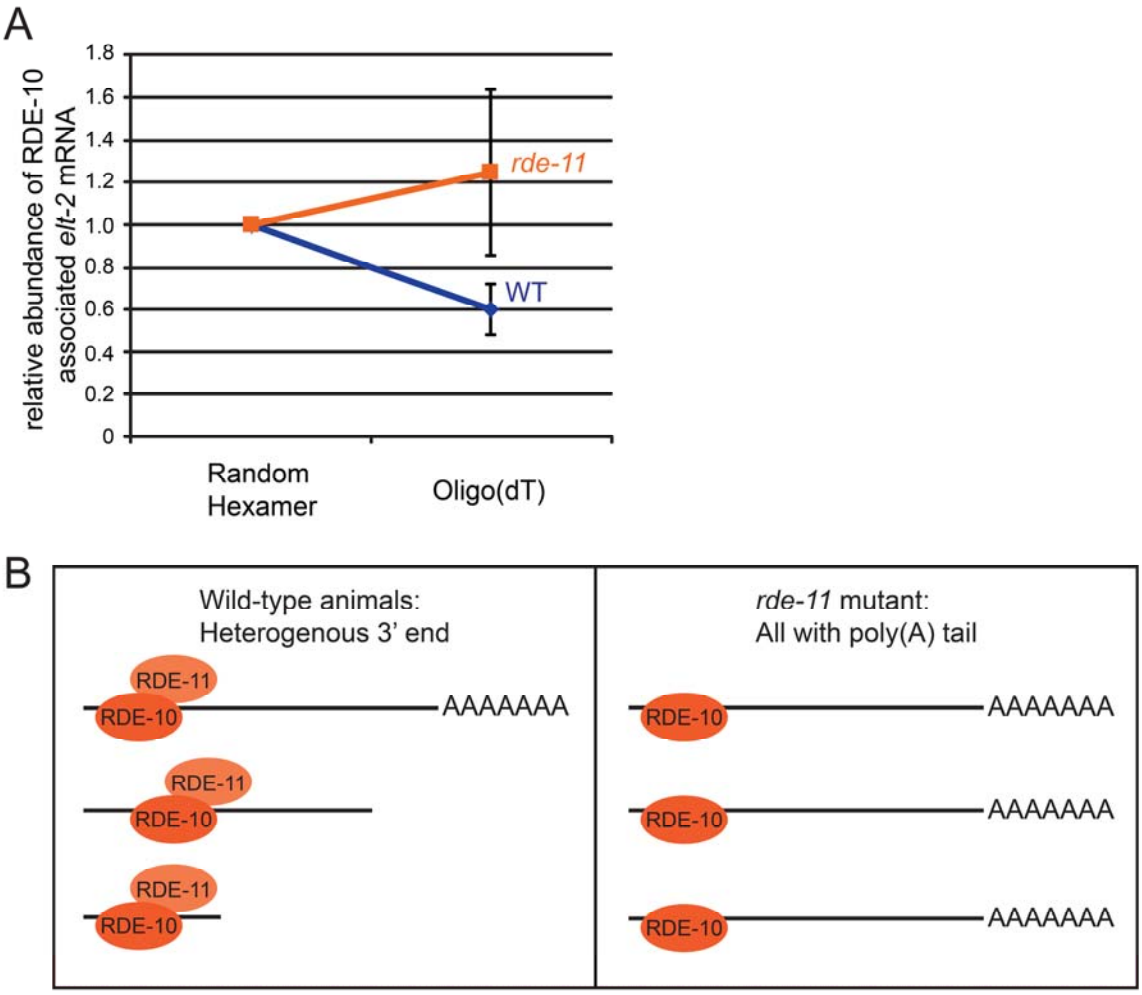

Figure 2.10. RDE-10 associates with target mRNAs that contain heterogeneous 3' ends. (A) The abundance of RDE-10 associated *elt-2* target mRNA in wild-type and *rde-11(hj37)* animals was measured by real-time PCR. RNA samples were reverse-transcribed using oligo(dT) or random hexamer primers and a region 5' to the RNAi trigger amplified. Reduced abundance of oligo(dT) primed products indicate a depletion of poly(A) tailed *elt-2* mRNA in wild-type but not *rde-11* mutant animals. The abundance of *elt-2* mRNA reverse transcribed by random hexamers was set as 1. Results are shown as mean ± standard deviation from at least three independent samples assayed in triplicates. (B) A model for RDE-10/RDE-11 triggered heterogeneity of target mRNA 3' ends. RDE-10 associated target mRNAs undergoes deadenylation and degradation in an RDE-11 dependent manner.

Figure 2.11. Exo-RNAi induced *elt-2* small RNA size and 5' nucleotide distribution in WT, *rde-10* and *rde-11* mutant. (A) Sense small RNA profile in 5'-to-trigger region. (B) Antisense small RNA profile in 5'-to-trigger region. (C) Sense small RNA profile in trigger region. (D) Antisense small RNA profile in trigger region. (E) Sense small RNA profile in 3'-to-trigger region. (F) Antisense small RNA profile in 3'-to-trigger region.

A

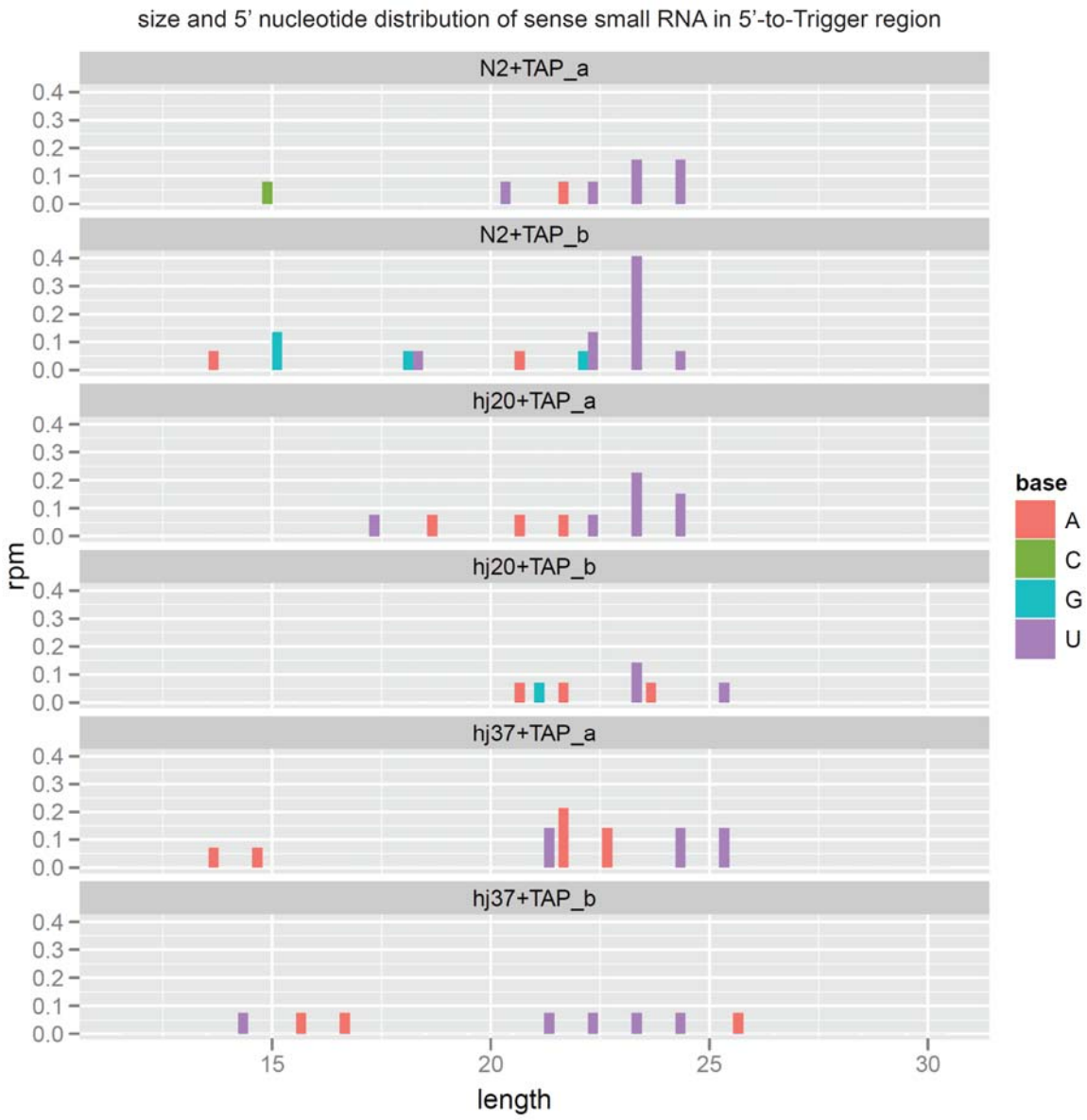

Figure 2.11. Exo-RNAi induced *elt-2* small RNA size and 5' nucleotide distribution in WT, *rde-10* and *rde-11* mutant.

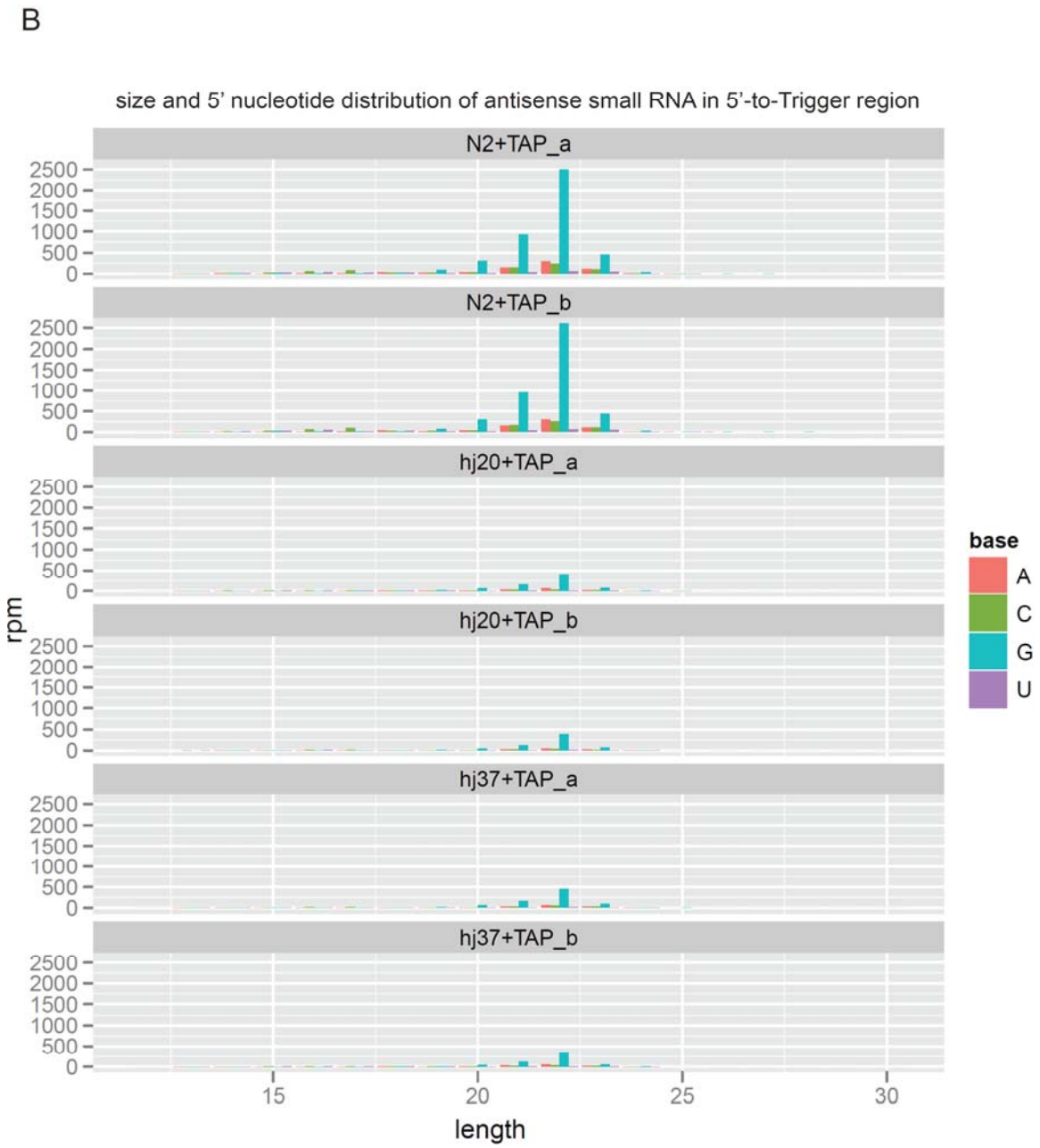

Figure 2.11. Exo-RNAi induced *elt-2* small RNA size and 5' nucleotide distribution in WT, *rde-10* and *rde-11* mutant.

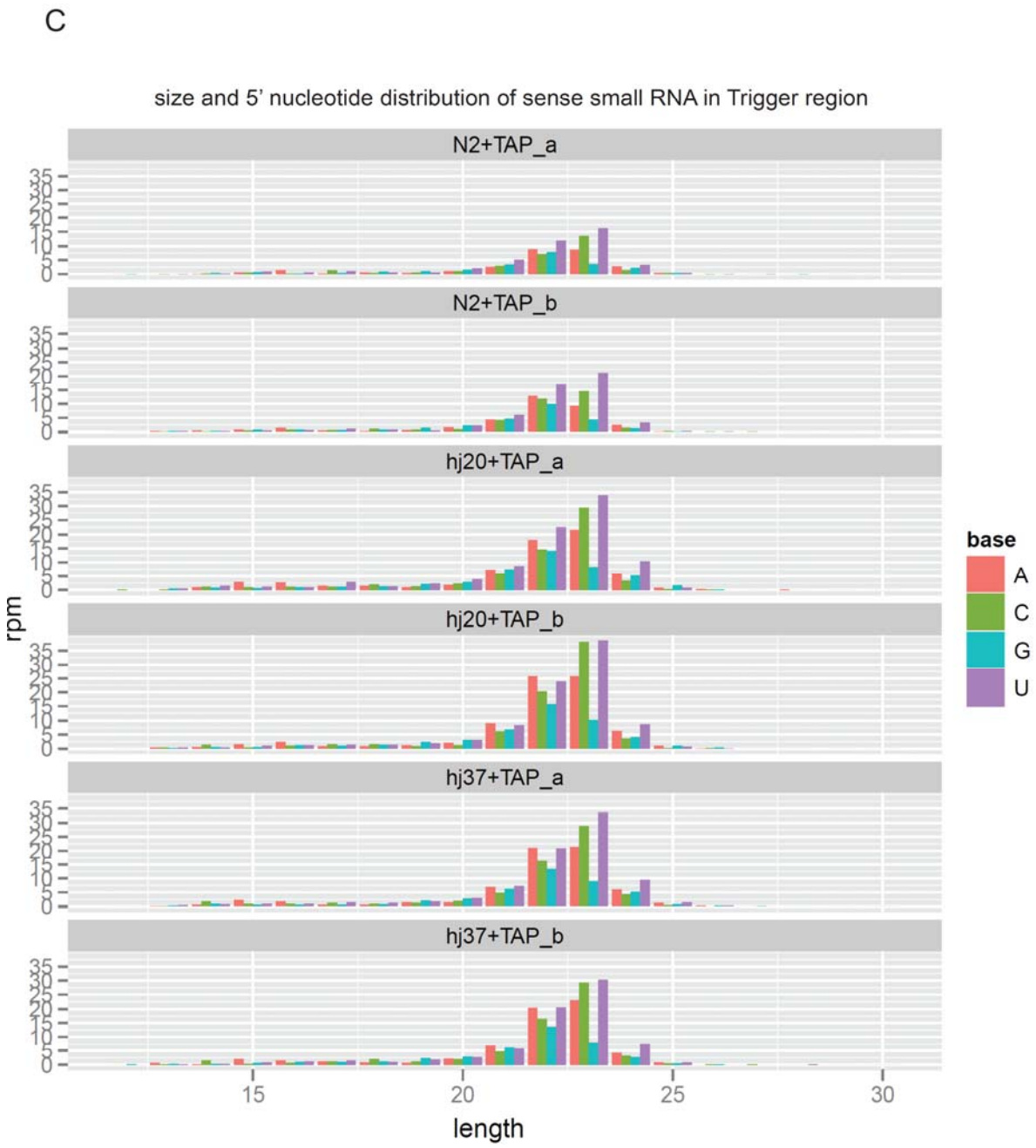

Figure 2.11. Exo-RNAi induced *elt-2* small RNA size and 5' nucleotide distribution in WT, *rde-10* and *rde-11* mutant.

D

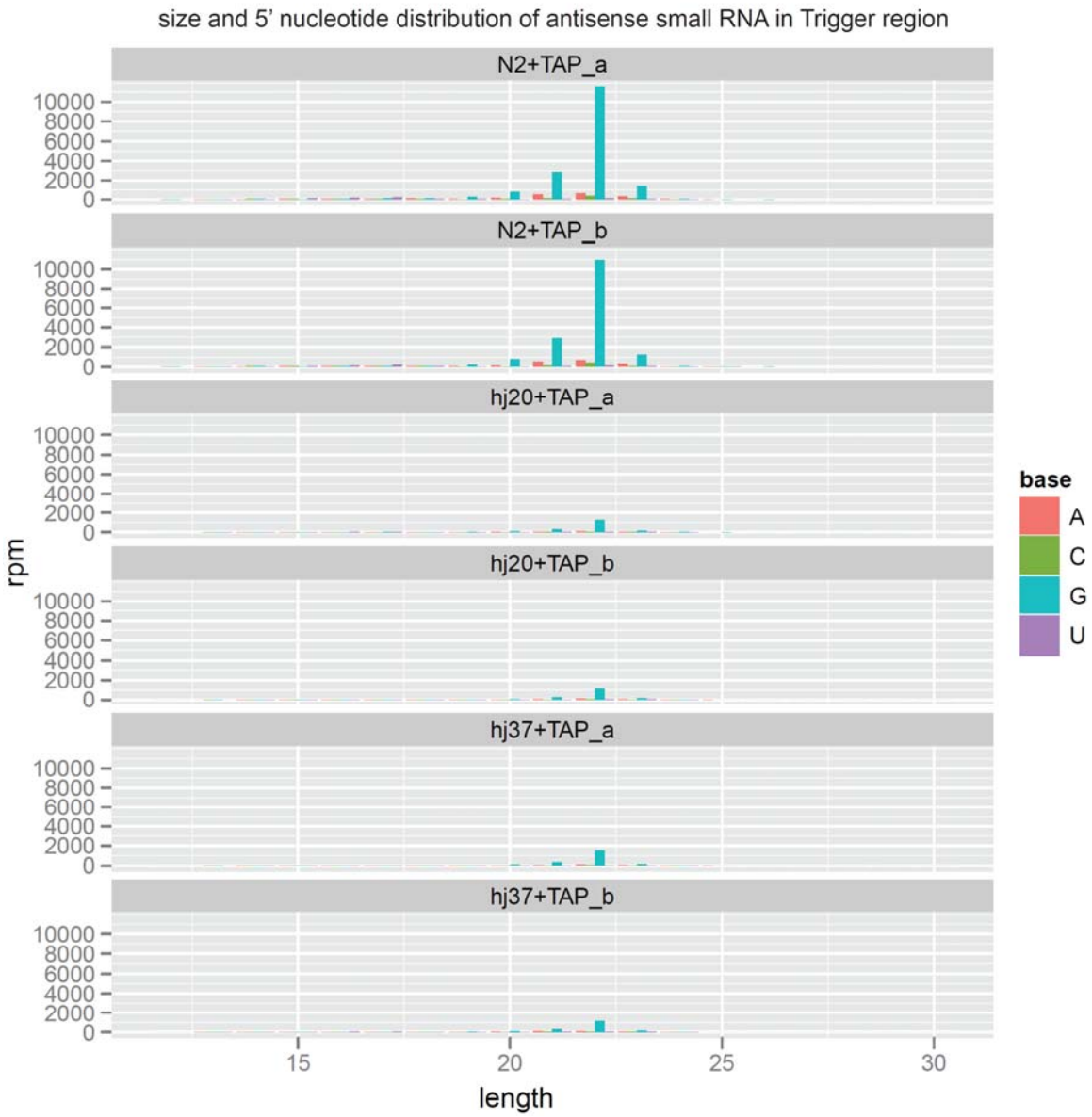

Figure 2.11. Exo-RNAi induced *elt-2* small RNA size and 5' nucleotide distribution in WT, *rde-10* and *rde-11* mutant.

E

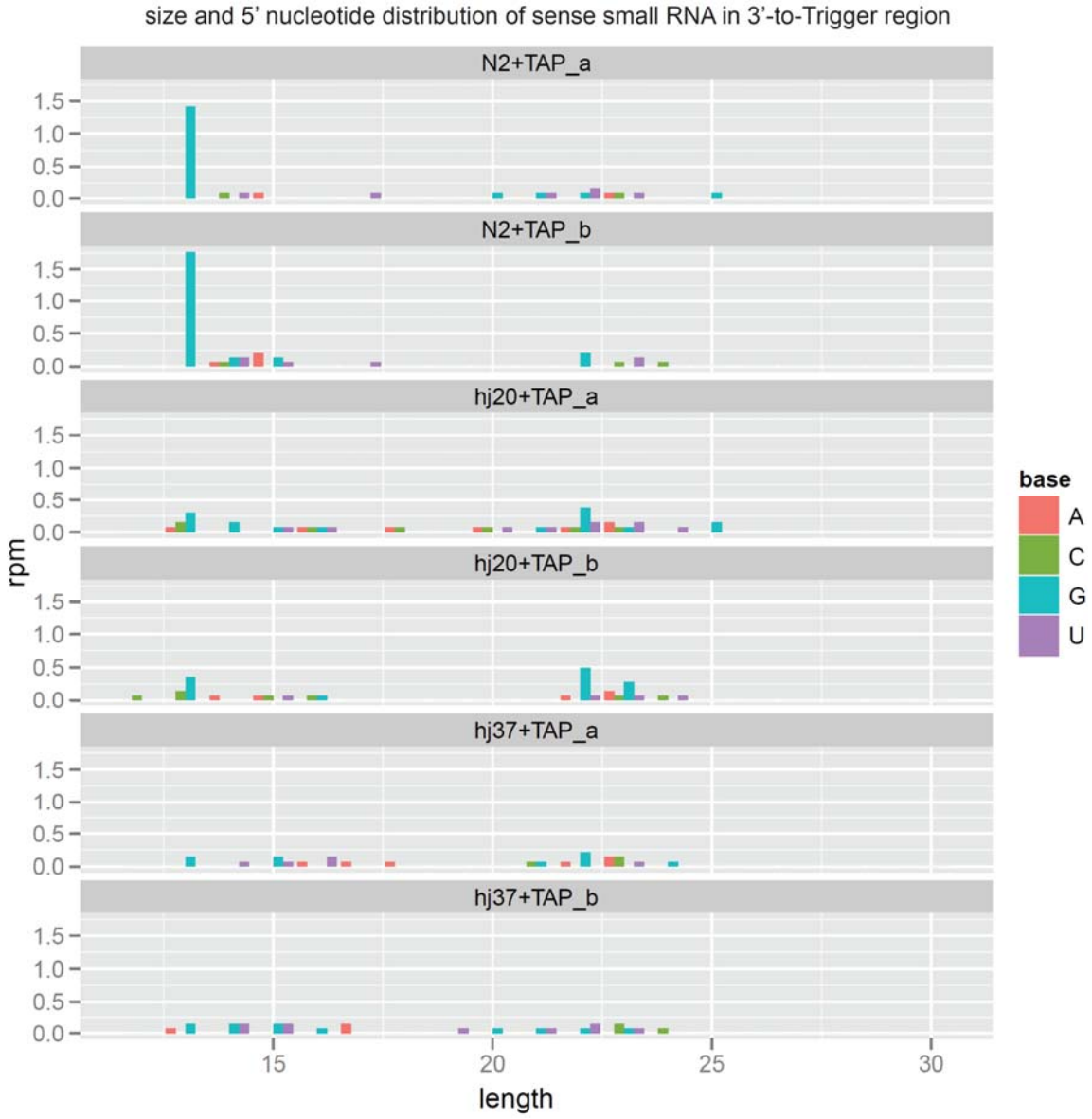

Figure 2.11. Exo-RNAi induced *elt-2* small RNA size and 5' nucleotide distribution in WT, *rde-10* and *rde-11* mutant.

F

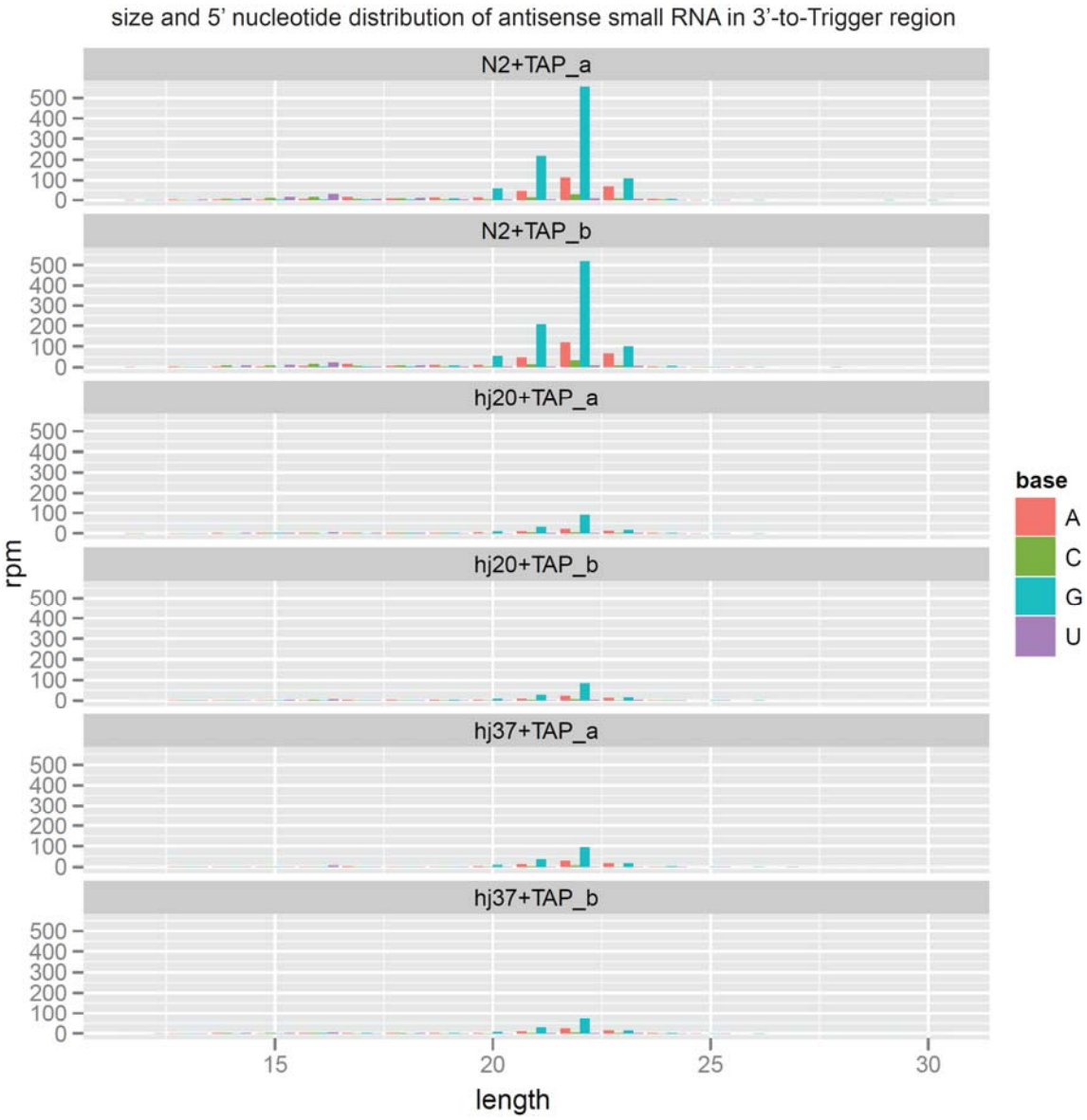

Figure 2.11. Exo-RNAi induced *elt-2* small RNA size and 5' nucleotide distribution in WT, *rde-10* and *rde-11* mutant.

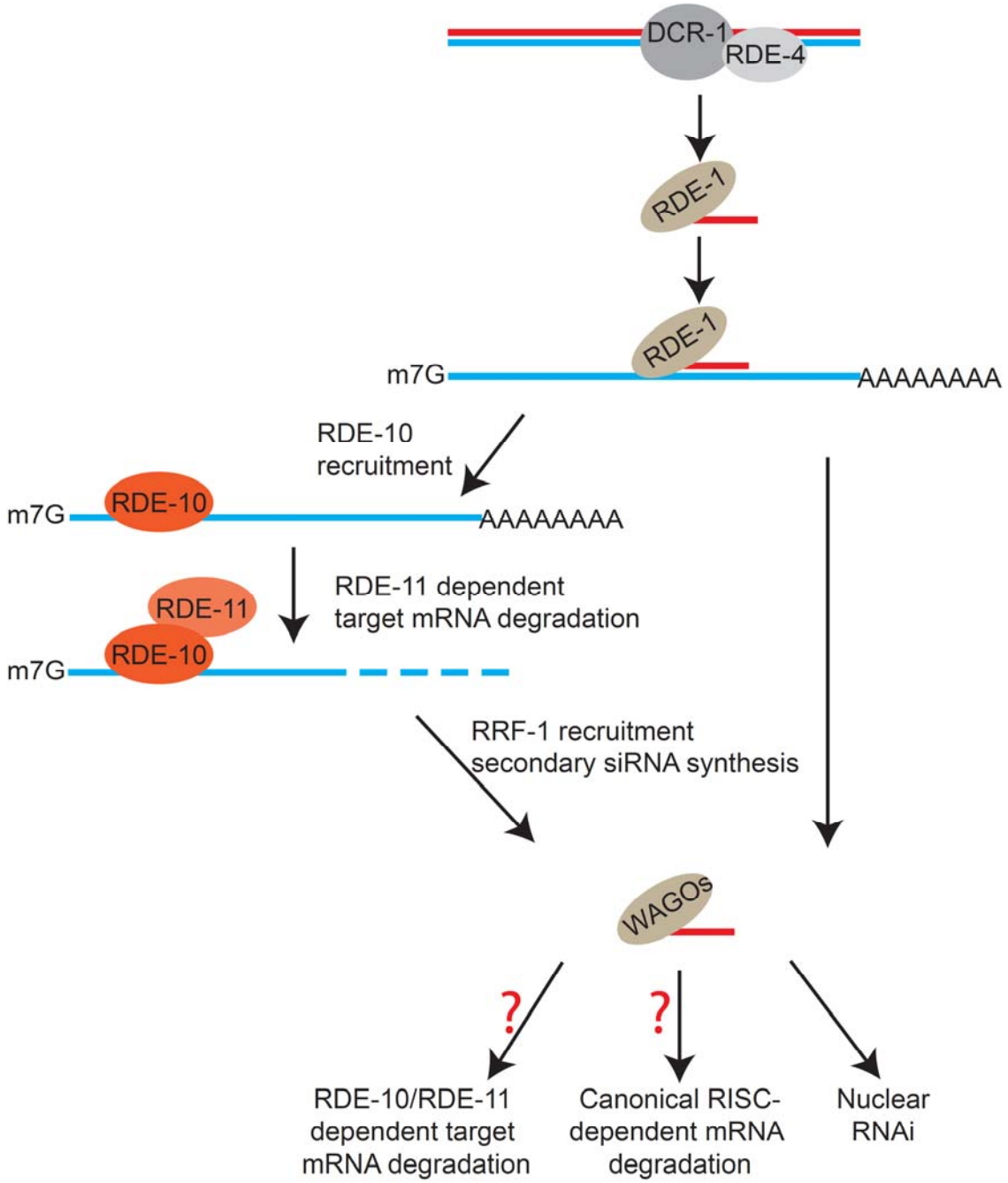

Figure 2.12. A model: RDE-10/RDE-11 complex in the exogenous RNAi pathway in *C. elegans*.

Table 2.1. Susceptibility of worms to RNAi

	E. coli mediated feeding RNAi					
	cytoplasmic RNAi + nuclear RNAi					nuclear RNAi
	pos-1	*nhr-23*	*elt-2*	*unc-15*	*unc-22*	*lir-1*
Genotype / **Phenotype**	embryonic lethality	molt defect	larval arrest	paralysis	twitcher	larval lethality
Wild type (N2)	++	++	++	++	++	++
rde-1(ne300)	-	-	-	-	-	-
rde-10(hj20)	-	-	-	-	+	+
rde-11(hj37)	-	-	-	-	+	+
nrde-3(gg66)	+/++	+	+	+/++	+/++	-
rde-10(hj20);rde-11(hj37)	-	-	-	-	+	+
rde-10(hj20);nrde-3(gg66)	-	-	-	-	-	-
rde-11(hj37);nrde-3(gg66)	-	-	-	-	-	-
rde-10(hj20);nrde-3(gg66);Is[nrde-3(+)]	-	-	-	-	+	+

Nematodes of the indicated genotype were grown on *E. coli* (HT115) expressing double stranded RNA at 20^{o}C. Strong phenotype of high penetrance was indicated by (++) and resistance to RNAi was indicated by (-). Observations were made from at least three independent experiments.

Table 2.2. Small RNAs in *sel-1* locus after RNAi treatment

		reads per million mapped reads					
		5' to trigger	5' to trigger	trigger	trigger	3' to trigger	3' to trigger
sample name	TAP treatment	sense	antisense	sense	antisense	sense	antisense
wild type		1.44	1,327.82	380.62	3,954.15	5.83	441.62
wild type		1.74	1,364.65	402.36	4,021.82	7.34	399.64
wild type	+	0.63	6,192.15	121.87	21,089.61	2.52	1,451.34
wild type	+	1.08	6,343.82	152.76	20,581.61	3.11	1,388.26
rde-10(hj20)		2.25	245.28	638.46	798.15	4.14	85.37
rde-10(hj20)		1.32	194.94	622.69	760.56	4.38	66.26
rde-10(hj20)	+	0.76	1,086.98	268.29	2,501.55	3.03	246.5
rde-10(hj20)	+	0.49	954.79	294.11	2,307.29	2.33	222.3
rde-11(hj37)		1.16	295.28	580.99	922.98	4.37	98.22
rde-11(hj37)		0.98	182.2	595.59	748.11	3.83	68.67
rde-11(hj37)	+	0.92	1,198.77	255.86	2,928.62	1.63	267.77
rde-11(hj37)	+	0.59	880.95	242.74	2,370.12	1.92	212.17

Deep sequencing results of 21-24nt small RNAs that mapped to the *sel-1* mRNA in wild-type and mutant animals undergoing *sel-1* RNAi.

Material and Methods

Strains and transgenes

The wild-type strain was Bristol N2. All animals were raised at 20^{o}C unless specified. The following alleles and transgenes were used:

LGI: *rde-10(hj18), rde-10(hj19), rde-10(hj20), rrf-1(pk1417)*

LGIV: *rde-11(hj37)*

LGV: *rde-1(ne300)*

LGX: *nrde-3(gg66)*

hjSi10[rde-10p::3xFLAG-TEV-GFP::rde-10]

Generated by MosSCI, outcrossed 2 times with N2.

hjSi28[rde-10p::3xFLAG-TEV-GFP]

Generated by MosSCI, outcrossed 2 times with N2.

hjSi116[rde-10p::rde-11::TEV-3xFLAG]

Generated by MosSCI, outcrossed 2 times with N2

hjIs21[vha-6p::atgl-1b cDNA::GFP]

Generated by UV irradiation, outcrossed 5 times with N2

ggIs1[nrde-3p::3xFLAG::GFP::nrde-3(+)]

a gift from Scott Kennedy

hjEx11[rde-10p::rde-11 cDNA::mCherry-3xHA] 20ng/ul

tub-1::gfp (20ng/µl) and pBluescript (60ng/µl) injected into *rde-11(hj37)*

hjEx12[rde-10p::rde-11 cDNA(C203S)::mCherry-3xHA] 20ng/ul

tub-1::gfp (20ng/µl) and pBluescript (60ng/µl) injected into *rde-11(hj37)*

Real-time PCR and primers

RNA was extracted using TRI reagent (Molecular Research Center) according to manufacturer's instructions. Genomic DNA contamination was removed using the TURBO DNA-free kit (AM1907, Ambion). cDNAs were synthesized using ImProm-II Reverse Transcription System (Promega). The cDNA was subject to real time PCR analysis using the IQ SYBR Green supermix (Bio-Rad) on an iCycler (Bio-Rad). Pimer sequences are described in Supplemental Material.

Primer pairs (sequence from 5' to 3') for real-time PCR used in this study were:

unc-15, ccagagagtccgcagatacc and ccgtgacgaaaatcttggag

unc-22, ggaatgttaagagctgtgactgg and gggtgctccaaagcttgat

gfp, tcagtggagagggtgaaggt and tcgagaagcattgaacacca

rpl-32, agggaattgataaccgtgtccgca and tgtaggactgcatgaggagcatgt

gpd-3, tggagccgactatgtcgttgag and gcagatggagcagagatgatgac

elt-2

5' coding region: ctccaattgaacggcaaagt and cggttgcatggtagtttggt

3' coding region: agctgggttgatgatggttc and ccgcagctttggtttcat

dpy-28

5' coding region: caaagtcgtcgattatctcgtt and caccaattccacatcgacac

3' coding region: gccttcataggcttcaagaca and catttttcgacgttgaatgc

flr-1

5' coding region: cttctactgggctatcatgcaa and tttgtggtgttcagagggttt

sel-1

5’ coding region: ctctggtatctgcggaagga and ctcatcttgctgtgatgtgacc

Specificity of primers was examined by melting curves and sequencing of PCR products. Primer efficiency was tested with a dilution series of the template.

Sequences used for small RNA analysis

mir-1: UGGAAUGUAAAGAAGUAUGUA

mir-66: CAUGACACUGAUUAGGGAUGUGA

let-7: UGAGGUAGUAGGTTGUAUAGUU

21UR-1: UGGUACGUACGUUAACCGUGC

F37D6.3: chrI:10,486,644-10,487,373

E01G4.5: chrII:13,472,179-13,473,970

hcp-1: chrV:6,593,675-6,599,690

Genetic Screen

We mutagenized *hjIs21* animals with ethyl methane-sulfonate (EMS) using standard procedures for mutants that expressed ATGL-1::GFP in the adult stage. We screened ~20,000 haploid genomes and isolated mutants that fell into at least three complementation groups. One of them was identified to be *rde-1*. Genetic mapping with the Hawaiian isolate CB4856 placed *rde-10(hj18)* on LGI between snp_Y47G6A and snp_T28F2. RNAi screen and candidate gene sequencing identified a C to T mutation which causes a single amino acid substitution (S228F) in

Y47G6A.4. *rde-10(hj19)* and *rde-10(hj20)*, both carrying a premature stop codon in Y47G6A.4, were later identified from this complementation group. We used *hj20* as the reference allele. *rde-11(hj37)* was mapped to an interval in LGIV that included B0564.11, which encoded a strong interacting partner of GFP::RDE-10. Sequencing of B0564.11 in *rde-11(hj37)* identified a G to A mutation that yields a premature stop codon. *rde-10(hj20)* and *rde-11(hj37)* were rescued by single copy transgenes *hjSi10* and *hjSi116*, respectively.

RNAi experiments

RNAi was carried out as previously reported (Timmons *et al.* 2001). Bacterial clones expressing dsRNA were obtained from the Ahringer RNAi library except for *dpy-28* (PCR product of 5'-cgaaacgtgcttcaactag-3' and 5'-atgtccatgtcgattattatcc-3'), *sel-1* (PCR product of 5'-tgcatggagccggaatcgga-3' and 5'-tgcatcggcacttcctgact-3') and *flr-1* (PCR product of 5'-ttggcagggaaaagctacat -3' and 5'-ctcctcctcagcaactgcat -3') RNAi clones. For *unc-15* and *unc-22* RNAi experiments, $10OD_{600}$ of bacteria was seeded on 100mm RNAi plates. Plates were left at room temperature overnight for dsRNA expression. 6000 eggs from egg preps were seeded on plates in triplicate for each strain. After 48 hrs at 20^{o}C, worms were washed extensively with M9 and RNA was extracted with TRI Reagent (Molecular Research Center). For *elt-2* RNAi experiments, 4000 synchronized L1 animals from egg preps were seeded on 100mm RNAi plates. Worms were collected after 46hrs at 20^{o}C and RNA was extracted with TRI Reagent.

Worm lysate preparation and immuno-precipitation for MudPIT

Mixed-stage worms grown in liquid culture with *E. coli* HB101 were used for preparation of worm lysate and immuno-precipitation. Worms were collected and washed extensively with M9,

ground in liquid Nitrogen and added to IP buffer (20mM HEPES-KOH[pH7.5], 10mM KOAc, 2mM $Mg(OAc)_2$, 110mM KCl, 0.1% NP-40, 1x Protease Inhibitor(Sigma, P8340)). 3xFLAG tagged RDE-10 was purified by immunoprecipitation with agarose beads conjugated with anti-FLAG antibodies. Immunoprecipitations were carried out at 4^{o}C for 4hrs. GFP::RDE-10 or GFP were eluted from beads by TEV protease treatment at 4^{o}C overnight in IP buffer.

Acetone-precipitated proteins were urea-denatured, reduced, alkylated and digested with endoproteinase Lys-C (Roche) followed by modified trypsin (Promega) as described (Florens and Washburn 2006). Fully automated 10-step MudPIT runs were carried out on a linear ion trap mass spectrometer (Thermo Fisher Scientific) equipped with a nano-LC electrospray ionization source. Tandem mass (MS/MS) spectra were interpreted using SEQUEST (Eng *et al.* 1994) against a database consisting of 23714 non-redundant *C. elegans* proteins (NCBI, 2010-03-12 release), 177 sequences for usual contaminants (such as keratins and proteolytic enzymes), as well as the sequences for FLAG-GFP and FLAG-GFP::RDE-10. In addition, to estimate false discovery rates (FDR), each non-redundant protein entry was randomized (keeping the same length and amino acid composition) and these "shuffled" sequences were added to the forward sequences and searched at the same time. Peptide/spectrum matches were sorted and selected using DTASelect (Tabb *et al.* 2002). FDRs at the protein and peptide levels were both less than 1%. To estimate relative protein levels, distributed Normalized Spectral Abundance Factors (dNSAFs) were calculated for each detected protein as described (Zhang *et al.* 2010).

RNA Immuno-precipitation

RDE-10 and RDE-11 RNA IP (RIP) were performed as previously described (Guang *et al.* 2008) with modifications. To isolate RDE-10 associated total RNAs after RNAi, synchronized L1

animals (from egg preps) were seeded onto 100mm RNAi plates and collected at L4 stage (~44-46hrs at 20^{o}C). Animals were sonicated in lysis buffer (20 mM Tris-HCl, pH 7.5, 200 mM NaCl, 2.5 mM $MgCl_2$, 0.5% NP-40, and 10% glycerol, with proteinase inhibitor tablet EDTA-free (Roche) and RNaseOUT (Invitrogen)). 3xFLAG::GFP::RDE-10 was immunoprecipitated with Dynabeads M280 pre-coated with anti-FLAG antibody (Sigma, F1804). After extensive washes, 3xFLAG::GFP::RDE-10 was eluted with 150 ug/mL 3xFLAG peptide. Eluates were first incubated with Turbo DNase I (Ambion) at 37^{o}C for 20 minutes. The RNAs were then purified by TRI Reagent, followed by isopropanol precipitation. cDNAs were generated from RNAs with ImProm-II Reverse Transcription System using a mixture of oligo(dT) and random hexamer primers. For Fig. 2.10, RNA samples were split into two and reverse transcription performed with either oligo(dT) or random hexamer primers. qPCRs were performed as described above. Target mRNA enrichment was normalized by non-specific binding of *gpd-3* mRNA. RDE-11 RIP was performed in the same way as RDE-10 RIP.

Antibodies

Monoclonal antibodies against the FLAG epitope (clone M2; Sigma) and HA epitope (clone 3F10; Roche) were used for Western blot. For immunoprecipitation anti-FLAG M2 Affinity Gel (A2220, Sigma) was used.

RDE-10/RDE-11 Co-IP

Strains used were *rde-10(hj20); hjSi10; hjEx11* and *hjSi28; hjEx11*. Worms were ground in liquid Nitrogen and added to IP buffer (20mM HEPES-KOH[pH7.5], 10mM KOAc, 2mM

$Mg(OAc)_2$, 110mM KCl, 0.1% NP-40, 1x Proteinase Inhibitor (Sigma, P8340)). 3xFLAG::GFP::RDE-10 or 3xFLAG::GFP proteins were immuno-precipitated with anti-FLAG beads at 4°C for 2hrs and washed twice in IP buffer. To digest nucleic acid, beads were treated with 20 units of Benzonase (Sigma, E8263) in 1mL IP buffer for 30mins at room temperature. Beads were washed twice more in IP buffer. Proteins on beads were then eluted with 2x SDS buffer. Eluates were subject to Western blotting.

In-vitro translation and pull-down assay

The *rde-10* and *rde-11* cDNAs were cloned into pcDNA3.1 for expression of RDE-10::FLAG and RDE-11::HA fusion proteins. RDE-10 and RDE-11 recombinant proteins were synthesized separately using TnT T7 Coupled Reticulocyte Lysate System (L4610, Promega). Lysates containing RDE-10 and RDE-11 recombinant proteins were mixed together and diluted with 3 volume of IP buffer (20mM HEPES-K[pH7.5], 50mM NaCl, 5mM MgCl2, 0.1% NP-40, with or without 50μM $ZnSO_4$) plus Roche proteinase inhibitor (EDTA-free). Mixtures were incubated at 37°C for 20mins and then incubated with anti-FLAG agarose beads (Sigma, A2220) at 4°C for 1.5hrs. Beads were washed five times with 800μl IP buffer. Proteins on beads were eluted using 2x SDS loading buffer. Eluates were subject to Western blotting.

Small RNA cloning and deep sequencing

Synchronized L1 worms were grown on RNAi plates seeded with HT115 *E. coli* expressing a *sel-1* RNAi trigger as previously described (Pak and Fire 2007). After 48hrs at 20°C, 40000 worms were washed 5 times with 10ml M9, and then homogenized in Tri-reagent. Samples were

kept at -80^{o}C. Purified total RNA were processed with MirVana kit (Invitrogen) for small RNA enrichment. Equal amount of small RNAs (20~30ug) were resolved on 15% TBE-Urea Acrylamide gels. Gels containing small RNAs of 21-24nt were cut out and purified with a small-RNA PAGE Recovery Kit (Zymo Research, R1070). Each small RNA sample was split into two (one for TAP treatment and another untreated) and processed with the ScriptMiner Small RNA-Seq Library Preparation Kit (Epicentre, SMMP1012). Libraries from different samples were indexed with RNA-Seq Barcode Primers (Epicentre, RSBC10948). Two biological samples of each condition (wild type, wild type + TAP, *rde-10* mutant, *rde-10* mutant + TAP, *rde-11* mutant and *rde-11* mutant + TAP) were used for library preparation. A total of 12 libraries were pooled together and subject to Illumina HiSeq-50bp single read deep sequencing. Sequencing reads were clipped with Fastx_clipper (v0.0.13) to remove adaptor sequence and aligned to the UCSC reference genome ce6 with Tophat (v1.4.0). The aligned reads ranged from 10.7 to 13.3 million for each library. The coverageBed component of BEDtools (v2.12.0) was used to count the reads of each region and small RNAs. RPMs were calculated by (reads_aligned_to_region / all_aligned_reads_for_sample) * 1000000. The data reported in this paper have been deposited in the Gene Expression Omnibus (GEO).

Tobacco acid pyrophosphatase (TAP) and Terminator exonuclease (TEX) treatment of RDE-10 bound target mRNA

Worms expressing FLAG-tagged RDE-10 (*rde-10;hjSi10*) were grown on *elt-2* RNAi plates and then subject to RNA-IP. After phase separation, the aqueous phase of Tri-reagent treated samples was further purified with RNA clean & Concentrator-5 Kit (Zymo Research, R1015). The

purified RNA in nuclease-free water was evenly split into four samples. 15 units of TAP (Epicentre, T19100) or equal volume of nuclease-free water were added to each sample in TAP reaction buffer (final volume 25µl). Samples were incubated at 37^{o}C for 1.5hrs. The RNA samples were then purified with RNA clean & Concentrator kit again. The TEX (Epicentre, TER51020) treatment was performed following vender's Buffer A protocol. After TEX treatment, RNAs were purified with RNA clean & Concentrator kit and converted to cDNA with ImProm-II Reverse Transcription System (Promega). This was followed by real-time PCR using primers that amplified the 5' coding region of *elt-2*. The relative amount of RNAs in each sample was normalized to the one without treatment.

Author contributions

This chapter was published in

Yang H, Zhang Y, Vallandingham J, Li H, Florens L, Mak HY. (2012). "The RDE-10/RDE-11 complex triggers RNAi-induced mRNA degradation by association with target mRNA in C. elegans." Genes Dev 26(8): 846-856 (Yang *et al.* 2012).

H.Y. was responsible for the design and execution of experiments in all Figures, Table 2.1 and Table 2.2. Y.Z. and L.F. performed MudPIT analysis for Fig. 2.5A. J.V. and H.L. performed deep sequencing data analysis for Fig. 2.8, Fig. 2.11 and Table 2.2. H.Y.M. conducted the genetic screen and contributed to experimental design. H.Y. and H.Y.M. wrote the manuscript. All authors have read and approved the manuscript and declared no conflicts of interest or competing financial interests.

Chapter 3

A putative RNA helicase RDE-12 engages target mRNA to promote RNAi response amplification in novel cytoplasmic foci in *C. elegans*

Abstract

In *C. elegans*, the RNAi response is enhanced through a unique process of siRNA amplification. The molecular mechanisms underlying such amplification are not completely understood. Argonaute protein RDE-1 binds primary siRNAs derived from dsRNA triggers and is guided to target mRNAs. This is followed by recruitment of RNA-dependent RNA polymerases (RdRPs) to synthesize secondary siRNA by using target mRNAs as templates. Here, through a genetic screen, we identified a putative DEAD-box RNA helicase, RDE-12, that functions upstream of RdRPs and downstream of RDE-1. RDE-12 engages target mRNAs and promotes secondary siRNA biogenesis in both the exogenous RNAi and the endogenous RNAi pathways. We further demonstrated that GFP::RDE-12 fusion protein forms cytoplasmic foci in the soma and resides in perinuclear P granules in the germline. Mutations that disrupt a nucleoporin domain and the catalytic residues of the helicase domain impair RDE-12 function *in vivo*. We hypothesize that RDE-12 may act as a link between mRNA targeting and secondary siRNA synthesis in the RNAi pathway.

Results and discussion

rde-12 is required for transgene silencing and RNAi in *C. elegans*

A transgene (*hjIs21*) expressing ATGL-1::GFP fusion protein undergoes a unique cycle of desilencing and silencing in every generation (Yang *et al.* 2012). In L4 animals, the GFP fusion is not detectable (Fig. 3.1A). We identified one mutant allele defining the gene *rde-12*, which is required for transgene silencing in the reporter strain *hjIs21* (Fig. 3.1A). From a genetic screen for mutants that are defective in transgene silencing, we identified the RDE-10/ RDE-11 protein complex that triggers RNAi-induced mRNA degradation by association with target mRNA (Yang *et al.* 2012). Here, we report the identification of *rde-12* from the same screen (Fig.3.1A). We initially identified one nonsense allele, *hj41*. From a genetic non-complementation screen, we identified three additional alleles of *rde-12* that failed to silence the reporter transgene (Fig.3.1B). *rde-12* encodes a putative DEAD-box RNA helicase with a nucleoporin domain at the C-terminus (Fig. 3.1B) (Altschul *et al.* 2005; Marchler-Bauer *et al.* 2011). The nucleoporin domain is rich in phenylalanine (F) and glycine (G), FG repeats, and found in nucleoporins that form the nuclear pore complex. In *C. elegans*, transgene silencing and RNAi share common factors (Kim *et al.* 2005). To test whether *rde-12* is required for RNAi, we performed RNAi to silence endogenous genes that are expressed in different tissues. *rde-12(-)* mutant animals fail to response to RNAi and can be rescued by single-copy transgenes expressing wild-type RDE-12 (Table 3.1). Taken together, our results indicate that *rde-12* is a novel gene required for transgene silencing and RNAi in *C. elegans*.

RDE-12 localized to cytoplasmic foci in soma and P granules in germline

RDE-12 was localized to P granules in the germline based on a high-copy transgene (Sheth *et al.* 2010). We established a single copy transgene that expressed fusion protein of green fluorescent protein (GFP) and full-length RDE-12. Expression of GFP::RDE-12 rescued the loss-of-function phenotypes of *rde-12(-)* mutant animals. GFP-RDE-12 is co-localized with P granules marker PGL-1 to perinuclear region in germline (Fig. 3.2A). P granules are germline specific cytoplasmic bodies with multiple putative functions. It has been proposed that P granules act as hydrophobic barriers that will slow down mRNAs diffusion when newly synthesized mRNAs exit nuclearpores and enter the cytoplasm (Sheth *et al.* 2010; Updike *et al.* 2011). The extended stay of mRNAs in P granules may allow regulatory factors (for example, Argonaute proteins) to find their target mRNAs. Multiple small regulatory RNA pathway components have been shown to localize to P granules (Updike and Strome 2010; Phillips *et al.* 2012). The localization of RDE-12 is consistent with its function in the germline RNAi pathway (Table 3.1). Though P granules are absent in the soma, GFP::RDE-12 remains and forms cytoplasmic foci. Processing bodies (P bodies) are cytoplasmic foci that are involved in mRNA degradation (Balagopal and Parker 2009). RNAi pathway components like Argonaute proteins were localized to P bodies (Sen and Blau 2005). Since RDE-12 is required for RNAi, it is possible that RDE-12 is localized to P bodies. Surprisingly, only a few RDE-12 foci overlapped with P bodies (Fig. 3.2B). Therefore, RDE-12 marks a population of cytoplasmic foci that are distinct from P bodies.

RDE-12 engages mRNAs targeted by RNAi

We showed that RDE-10/11 protein complex associates with target mRNAs that are undergoing degradation (Yang *et al.* 2012). Since RDE-12 is predicted to be an RNA helicase, we hypothesize that RDE-12 may also associate with target mRNAs. To test this possibility, we performed RNA co-immunoprecipitation to examine whether RDE-12 can engage target mRNAs in response to exogenous RNAi. The *elt-2* mRNA level was reduced by 80% after RNAi knock down (Yang *et al.* 2012). Despite low abundance of the *elt-2* mRNA, we detected ~130-fold more of the *elt-2* mRNA bound by RDE-12 (Fig. 3.3A). Similar result was observed when *dpy-28* was targeted by RNAi (Fig. 3.3A).

To test whether RDE-12 requires siRNA for target mRNA recognition, we also performed RDE-12 RNA IP in *rde-1(-)* and *rrf-1(-)* animals. While *rde-1(-)* animals are defective in primary and secondary siRNA biogenesis (Tabara *et al.* 2002; Pak *et al.* 2012), *rrf-1(-)* animals are defective in generating secondary siRNA in somatic tissues (Pak *et al.* 2012). We found that RDE-12 failed to associate with *flr-1* target mRNAs in *rde-1(-)* animals (Fig 3.3B). In contrast, RDE-12 was still able to engage target mRNAs in *rrf-1(-)* animals (Fig 3.3B). We previously showed that *rde-10(-)* animals were also partially defective in secondary siRNA biogenesis (Yang *et al.* 2012). We observed similar association of RDE-12 with target mRNA in *rde-10(-)* animals (Fig 3.3B) which suggested RDE-12 act upstream of RDE-10. Taken together, our results indicate that RDE-12 depends on primary but not secondary siRNA to engage target mRNAs and support a model that RDE-12 act downstream from RDE-1 and upstream of RDE-10 and RRF-1.

RDE-12 is required for secondary siRNA biogenesis

Our analysis so far placed RDE-12 at a step between RDE-1 and RRF-1 in the exogenous RNAi pathway in *C. elegans*. It is conceivable that the RDE-12 complex is required for amplification of the RNAi response. To test this hypothesis, we subjected wild-type and *rde-12(-)* mutant animals to RNAi against a somatic gene, *sel-1,* using a well-characterized trigger (Fig. 3.4A) (Pak and Fire 2007). We then purified small RNAs (~20 to 26 nucleotides) from duplicate populations of animals and profiled small RNAs by deep sequencing. Each biological sample yielded on average 21 million reads. The abundance of primary siRNAs was comparable in wild-type and *rde-12(-)* mutant animals (Fig. 3.4A). In contrast, about 50-fold decrease in secondary siRNAs was observed in *rde-12(-)* mutant animals (Fig. 3.4B). It is conceivable that the residual secondary siRNAs can be loaded to secondary Argonautes (WAGOs) to sustain low level of RNAi effect. Taken together, our results strongly suggest that RDE-12 is required for the secondary siRNA synthesis, which is critical for amplifying the exogenous RNAi response.

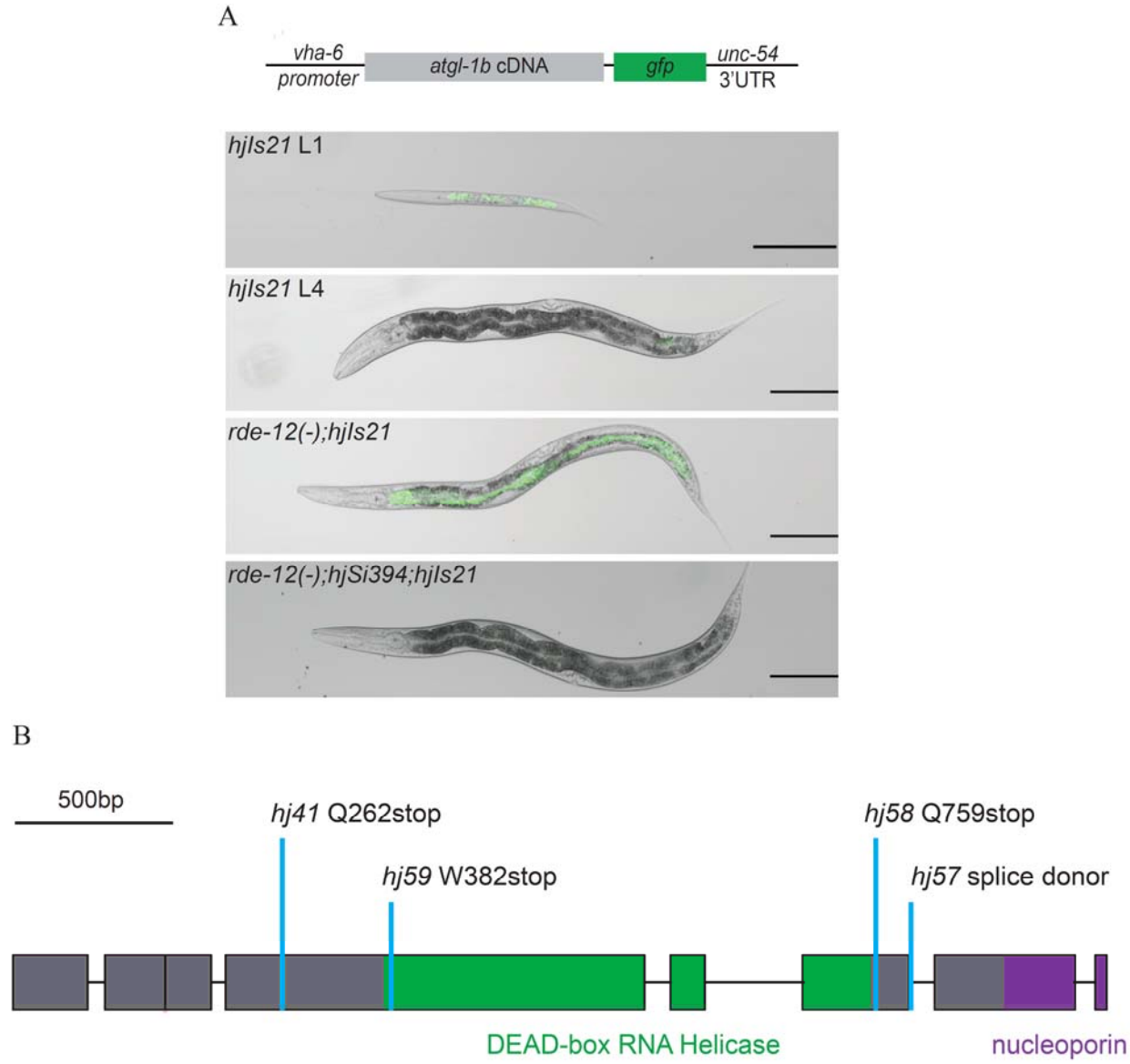

Figure 3.1. RDE-12 is a putative DEAD-box RNA helicase that required for transgene silencing. (A) Schematic representation of the *vha-6p::atgl-1b::gfp* transgene (*hjIs21*). Images of larval stage L4 wild-type animals carrying *hjIs21* are shown, together with *rde-12(hj41)* L4 mutant animals carrying the same transgene. Scale bar, 100µm. (B) Gene structures of *rde-12*. Mutant alleles and corresponding changes in protein coding sequences are indicated. Helicase core domain is highlighted in green and nucleoporin domain is highlighted in purple.

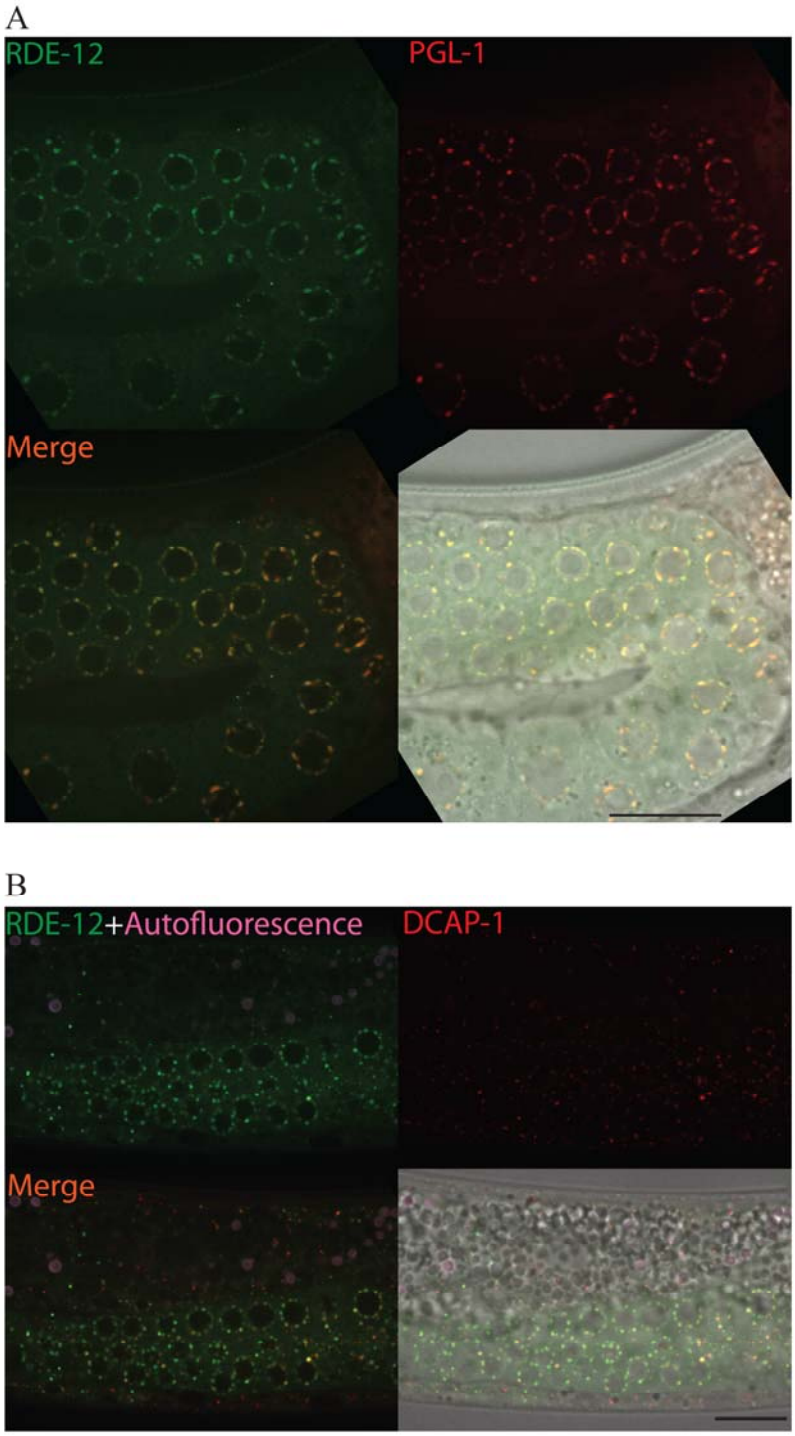

Figure 3.2. RDE-12 localized in cytoplasmic foci in soma and P granules in germline. (A) germline showing co-localization of GFP::RDE-12 with P granules maker mRuby::PGL-1. (B) Partial co-localization of GFP::RDE-12with P bodies marker mRuby::DCAP-1. Autofluorescence in intestinal cells is in purple. Bar, 10um

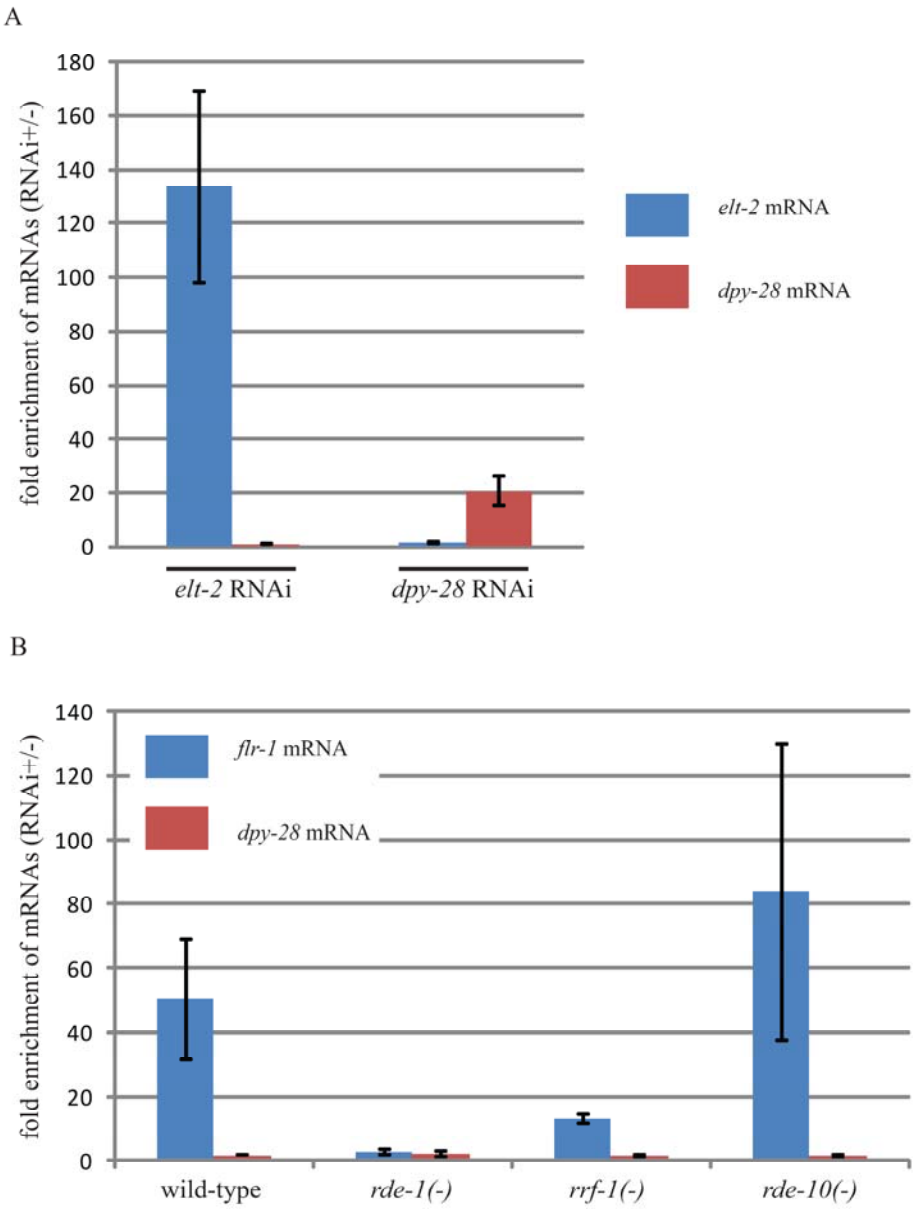

Figure 3.3. RDE-12 associates with mRNA targeted by RNAi. (A) Animals were subjected to elt-2 and dpy-28 RNAi separately. Target mRNAs, but not the nonspecific mRNA, preferentially associated with RDE-12. (B) Animals were subjected to flr-1 RNAi. Target mRNAs preferentially associated with RDE-12 in wild-type, rrf-1(pk1417), rde-10(hj20) but not rde-1(ne300) animals.

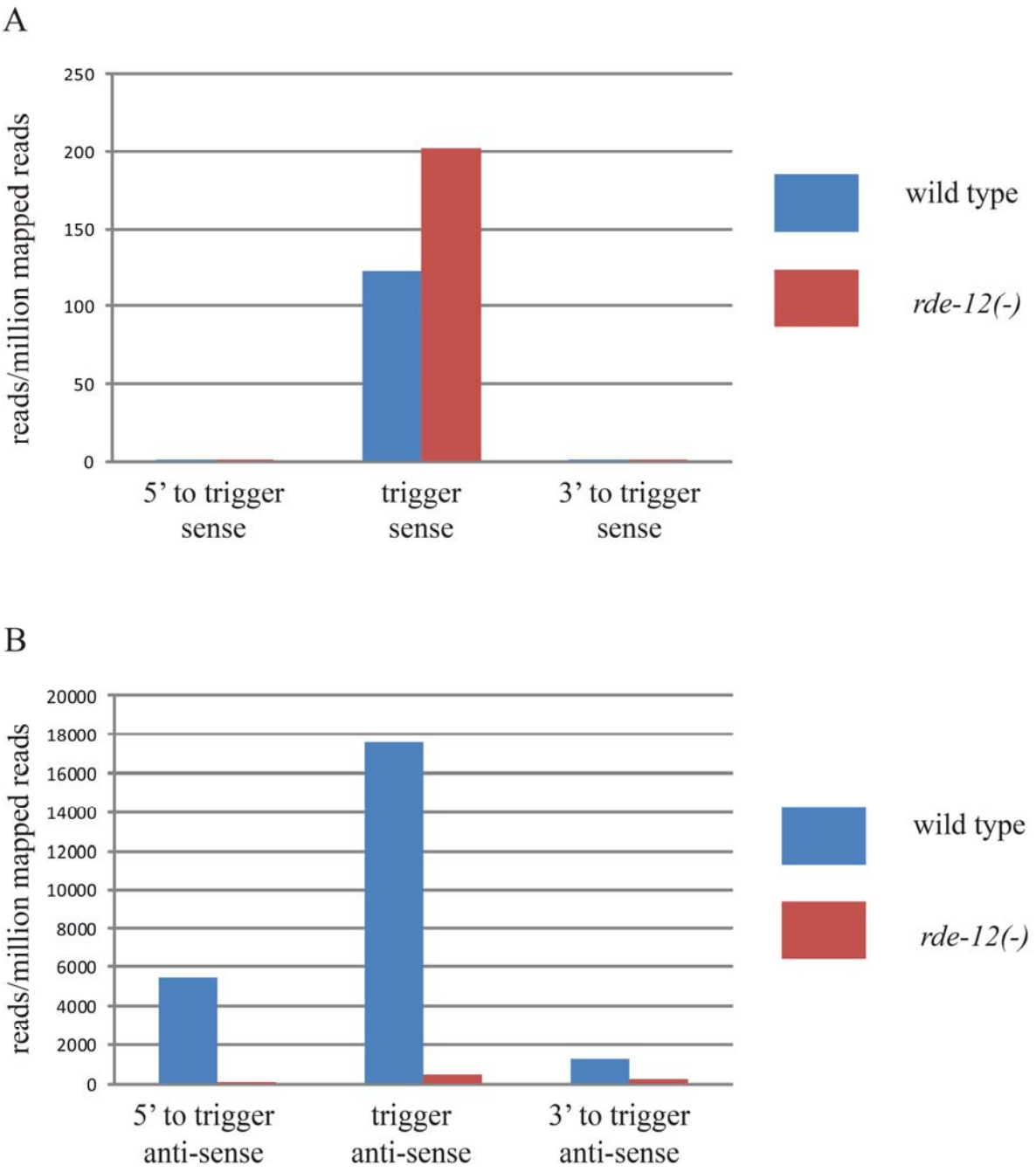

Figure 3.4. RDE-12 is required for secondary siRNA synthesis. The mean abundance of reads from two independent populations of animals undergoing *sel-1* RNAi is shown. (A) Sense *sel-1* siRNAs reads. (B) Antisense *sel-1* siRNAs reads.

Table 3.1. Susceptibility of worms to RNAi

	E. coli-mediated feeding RNAi		
	pos-1	*nhr-23*	*unc-15*
	embryonic lethality	*molt defect*	*paralysis*
Wild type	++	++	++
rde-1(ne300)	–	–	–
rde-12(hj41)	–	–	–
rde-12(hj41);hjSi394[rde-12(+)]	++	++	++
rde-12(hj41);hjSi395[rde-12(+)]	++	++	++

Nematodes of the indicated genotype were grown on *E. coli* (HT115) expressing double stranded RNA at 20^{o}C. Strong phenotype of high penetrance was indicated by (++) and resistance to RNAi was indicated by (-).

Material and Methods

Strains and transgenes

The wild-type strain was Bristol N2. All animals were raised at 20^{o}C unless specified. The following alleles and transgenes were used:

LGI: *rde-10(hj18), rrf-1(pk1417)*

LGV: *rde-1(ne300), rde-12(hj41)*

hjSi394[letm-1p::3xFLAG_TEV::rde-12]

Generated by MosSCI (LG II), outcrossed 2 times with N2.

hjSi395[dpy-30p::gfp::rde-12]

Generated by MosSCI (LG II), outcrossed 2 times with N2.

hjSi396[dpy-30p::mRuby::pgl-1]

Generated by MosSCI (LG I), outcrossed 2 times with N2

hjSi397[dpy-30p::mRuby::dcap-1]

Generated by MosSCI (LG I), outcrossed 2 times with N2

hjIs21[vha-6p::atgl-1b cDNA::GFP]

Generated by UV irradiation (LG X), outcrossed 5 times with N2

Real-time PCR and primers

RNA was extracted using TRI reagent (Molecular Research Center) according to manufacturer's instructions. Genomic DNA contamination was removed using the TURBO DNA-free kit (AM1907, Ambion). cDNAs were synthesized using ImProm-II Reverse Transcription System (Promega). The cDNA was subject to real time PCR analysis using the IQ SYBR Green

supermix (Bio-Rad) on an iCycler (Bio-Rad). Pimer sequences are described in Supplemental Material.

Primer pairs (sequence from 5' to 3') for real-time PCR used in this study were:

gpd-3, tggagccgactatgtcgttgag and gcagatggagcagagatgatgac

elt-2

5' coding region: ctccaattgaacggcaaagt and cggttgcatggtagtttggt

dpy-28

5' coding region: caaagtcgtcgattatctcgtt and caccaattccacatcgacac

flr-1

5' coding region: cttctactgggctatcatgcaa and tttgtggtgttcagagggttt

sel-1

5' coding region: ctctggtatctgcggaagga and ctcatcttgctgtgatgtgacc

Specificity of primers was examined by melting curves and sequencing of PCR products. Primer efficiency was tested with a dilution series of the template.

Genetic Screen

We mutagenized *hjIs21* animals with ethyl methane-sulfonate (EMS) using standard procedures for mutants that expressed ATGL-1::GFP in the adult stage. We screened ~20,000 haploid genomes and isolated mutants that fell into at least three complementation groups. One of them was identified to be *rde-1*. Genetic mapping with the Hawaiian isolate CB4856 placed *rde-12(hj41)* on LGV. RNAi screen and candidate gene sequencing identified a C to T mutation

which causes a premature stop in F58G11.2. Then we performed a non-complementation screen for additional alleles of *rde-12*. At the end we identified two more non-sense alleles and one allele with mutation at splice donor (*hj57, hj58* and *hj59*).We used *hj41* as the reference allele.

RNAi experiments

RNAi was carried out as previously reported (Timmons *et al.* 2001). Bacterial clones expressing dsRNA were obtained from the Ahringer RNAi library except for *dpy-28* (PCR product of 5'-cgaaacgtgcttcaactag-3' and 5'-atgtccatgtcgattattatcc-3'), *sel-1* (PCR product of 5'-tgcatggagccggaatcgga-3' and 5'-tgcatcggcacttcctgact-3') and *flr-1* (PCR product of 5'-ttggcagggaaaagctacat -3' and 5'-ctcctcctcagcaactgcat -3') RNAi clones.

RNA Immuno-precipitation

RDE-12 RNA IP (RIP) were performed as previously described (Guang *et al.* 2008) with modifications. To isolate RDE-12 associated total RNAs after RNAi, synchronized L1 animals (from egg preps) were seeded onto 100mm RNAi plates and collected at L4 stage (~42hrs at 20^{o}C). Animals were sonicated in lysis buffer (20 mM Tris-HCl, pH 7.5, 200 mM NaCl, 2.5 mM $MgCl_2$, 0.5% NP-40, and 10% glycerol, with proteinase inhibitor tablet EDTA-free (Roche) and RNaseOUT (Invitrogen)). 3xFLAG::RDE-12 was immunoprecipitated with Dynabeads M280 pre-coated with anti-FLAG antibody (Sigma, F1804). After extensive washes, 3xFLAG::RDE-12 was eluted with 150 ug/mL 3xFLAG peptide. Eluates were first incubated with Turbo DNase I (Ambion) at 37^{o}C for 20 minutes. The RNAs were then purified by TRI Reagent, followed by isopropanol precipitation. cDNAs were generated from RNAs with ImProm-II Reverse Transcription System using a mixture of oligo(dT) and random hexamer primers. qPCRs were

performed as described above. Target mRNA enrichment was normalized by non-specific binding of *gpd-3* mRNA.

Antibodies

Monoclonal antibodies against the FLAG epitope (clone M2; Sigma) were used for IP and Western blot. For immunoprecipitation anti-FLAG M2 Affinity Gel (A2220, Sigma) was used.

Small RNA cloning and deep sequencing

Synchronized L1 worms were grown on RNAi plates seeded with HT115 *E. coli* expressing a *sel-1* RNAi trigger as previously described (Pak and Fire 2007). After 48hrs at 20^{o}C, 40000 worms were washed 5 times with 10ml M9, and then homogenized in Tri-reagent. Samples were kept at -80^{o}C. Purified total RNA were processed with MirVana kit (Invitrogen) for small RNA enrichment. Equal amount of small RNAs (20~30ug) were resolved on 15% TBE-Urea Acrylamide gels. Gels containing small RNAs of 21-24nt were cut out and purified with a small-RNA PAGE Recovery Kit (Zymo Research, R1070). Each small RNA sample was split into two (one for TAP treatment and another untreated) and processed with the ScriptMiner Small RNA-Seq Library Preparation Kit (Epicentre, SMMP1012). Libraries from different samples were indexed with RNA-Seq Barcode Primers (Epicentre, RSBC10948). Two biological samples of each condition (wild type, *rde-12* mutant, wild type+RNAi and *rde-12* mutant+RNAi) were used for library preparation. A total of 8 libraries were pooled together and subject to Illumina HiSeq-

50bp single read deep sequencing. Sequencing reads were clipped with Fastx_clipper (v0.0.13) to remove adaptor sequence and aligned to the UCSC reference genome ce6 with Tophat (v1.4.0). The aligned reads ranged from 20.0 to 24.1 million for each library. The coverageBed component of BEDtools (v2.12.0) was used to count the reads of each region and small RNAs. RPMs were calculated by (reads_aligned_to_region / all_aligned_reads_for_sample) * 1000000.

Chapter 4

Conclusion and perspective

In the work described here, we identified the divergent RDE-10/RDE-11 complex as an essential output for exogenous RNAi in *C. elegans*. Our genetic, proteomic and biochemical data indicate that the RDE-10/RDE-11 complex is recruited to target mRNAs for their degradation, downstream of the Argonaute RDE-1 and primary siRNA biogenesis. Recruitment of the RDE-10/RDE-11 complex also plays an important role in supporting secondary siRNA synthesis. Taken together, the RDE-10/RDE-11 complex links the amplification of the RNAi response to the initial processing and utilization of the exogenous double-stranded RNA triggers (Fig. 2.12).

Multiple parallel pathways may operate downstream of the primary RNAi response that is dependent on DCR-1/dicer, RDE-1, RDE-4 and their associated proteins (Tabara *et al.* 2002; Duchaine *et al.* 2006; Yigit *et al.* 2006). Although the RNAi response in *rde-10* and *rde-11* mutant animals is severely blunted, the quantitative analysis of target mRNAs suggests that additional RNAi outputs remain operational. This can be attributed to residual secondary siRNA synthesis in *rde-10* and *rde-11* mutant animals. We postulate that recruitment of RRF-1 to target mRNAs, which is required for secondary siRNA synthesis, is strongly promoted by prior engagement of the RDE-10/RDE-11 complex to target mRNAs. However, RRF-1 may be recruited by additional mechanisms, perhaps through recognition of RDE-1 that is bound to target mRNAs. We note that high concentration of exogenous double-stranded RNA triggers introduced by injection (Chi Zhang and Gary Ruvkun, personal communications) and certain RNAi triggers introduced by feeding (e.g. *unc-22*) can partially bypass the requirement for RDE-10 and RDE-11. It is plausible that enhancement of RDE-1 association with target mRNAs, either through unusually strong primary siRNA-mRNA base-pairing or by high concentration of primary siRNAs, is sufficient for recruitment of RRF-1 to target mRNAs.

How does the RDE-10/RDE-11 complex promote secondary siRNA synthesis? RRF-1 may be recruited to the target mRNAs through protein-protein interactions. Such interactions may be transient since we did not detect RRF-1 in our proteomic analysis of RDE-10 associated proteins. We also consider an alternative scenario. At the initial phase of exogenous RNAi, a fine balance must be maintained between degradation and retention of target mRNAs. This is because if target mRNAs are degraded too rapidly, no template will be available for RRF-1 to synthesize secondary siRNAs. The RDE-10/RDE-11 complex preferentially associates with the region 5' to the RNAi trigger, in target mRNAs that are 5' capped (Fig. 2.7F) but lack a poly(A) tail (Fig.2.7D and Fig. 2.10). We therefore hypothesize that the RDE-10/RDE-11 complex generates and stabilizes partially degraded target mRNAs, which facilitates RRF-1 recruitment and/or its synthesis of secondary siRNAs.

Our deep sequencing analysis of small RNAs indicates that RDE-10 and RDE-11 are required for secondary siRNA synthesis, which is crucial for exogenous RNAi. In contrast, RDE-10 and RDE-11 are dispensable for the synthesis of selected endogenous siRNAs and micro-RNAs (Fig. 2.8D and E). This is in agreement with a more comprehensive survey of endogenous small RNAs in *rde-10* and *rde-11* mutant animals, which reveals the depletion of a small subset of endogenous siRNAs (Chi Zhang and Gary Ruvkun, personal communications). It is conceivable that the synthesis of endogenous secondary siRNAs is promoted by functional paralogs of RDE-10 and RDE-11 in *C. elegans*.

The specificity of the RNAi pathway is dictated by base pairing between target mRNAs and siRNA bound by Argonaute proteins. Both RDE-10 and RDE-11 can be recruited to target mRNA specifically. However, we did not detect any Argonaute family members in the

exogenous RNAi pathway as RDE-10 interacting proteins in our proteomic analysis. One possible reason is that the interaction between RDE-10 and Argonautes is too transient to be captured under our immunoprecipitation conditions. Or this could suggest a "drop off" model: once recognized by an Argonaute-containing complex, target mRNAs are labeled and then dropped off at a subcellular compartment where RDE-10/RDE-11 dependent degradation takes place. The "label" could be a protein (e.g. RSD-2 or RDE-10) or modifications of target mRNAs at their 5' or 3' end.

Although multiple models exist in other organisms, it is currently unknown if target mRNA degradation by RNAi in *C. elegans* is initiated by deadenylation, which is followed by 3' → 5' degradation by the exosome and/or 5' → 3' degradation initiated by de-capping. Alternatively, endonucleolytic cleavage within the target mRNA could be the initial step of degradation. We found that RDE-10 associated target mRNAs retained a 5' cap structure (Fig. 2.7F). Therefore, it was unlikely that the RDE-10/RDE-11 complex would promote de-capping. It is plausible that RDE-11 could instigate target mRNA degradation through recruitment of additional factors. Although a handful of conserved RISC components have been identified in *C. elegans*, they have only been reported to act in microRNA mediated gene silencing but not in RNAi (Caudy *et al.* 2003). Therefore, the RDE-10/RDE-11 complex may operate in conjunction of RISC in *C. elegans*. This is compatible with a previously proposed two-step model for RNAi in *C. elegans* (Yigit *et al.* 2006). The pioneering rounds of target mRNA degradation can be carried out by primary siRNA directed RDE-10/RDE-11 complex (Fig. 2.12), which is followed by full gene silencing by secondary siRNA directed RISC complex and nuclear RNAi apparatus. Nevertheless, we cannot rule out the possibility that the RDE-10/RDE-11 complex is required in additional gene silencing mechanisms subsequent to secondary siRNA synthesis (Fig. 2.12).

In *C. elegans* and plants, amplification of small RNAs is critical for potent endogenous and exogenous RNAi response and anti-viral immunity (Chapman and Carrington 2007; Ding 2010). Although conserved proteins such as Argonautes and RNA-dependent RNA polymerases are clearly involved, the precise mechanism of amplification differs. We propose that the divergence of the exogenous RNAi pathway in *C. elegans* can in part be attributed to its dependence on the RDE-10/RDE-11 complex. Further analysis of the *C. elegans* RNAi pathways should yield insights into how small RNA based regulation of gene expression can drift through evolution and provide clues on how to improve the efficiency of RNAi in heterologous systems.

RDE-12 is predicted to be an ATP-dependent DEAD-box RNA helicase. We showed here that GFP::RDE-12 was localized to P granules. P granules are considered as multifunctional compartments rather than single function compartments. Diverse proteins are enriched in P granules such as components of the spliceosome (Sm proteins); components of the RNAi pathway (CSR-1, DRH-3); PGL-1, a protein that binds an isoform of the mRNA cap-binding protein eIF4E (Sheth *et al.* 2010). So the localization of RDE-12 suggests that RDE-12 is likely to be involved in RNA metabolism. Indeed, we found that RDE-12 is required for RNAi and engages target mRNAs in response to RNAi. Our results successfully proved the connection between RDE-12's function and its subcellular localization.

DEAD-box RNA helicases are found to catalyze different biochemical activities: RNA duplex unwinding, protein displacement from RNA and strand annealing. So it is hard to predict the exact function of RDE-12 based on its homology to other RNA helicases (Jankowsky and Fairman 2007). However, RNA helicases are generally thought to function in the context of

larger RNP complexes, where the helicases interact with other cellular proteins. Therefore, to define the function of RDE-12, it is crucial for us to find out what RNA molecules and proteins are interacting with RDE-12. We showed that RDE-12 engages target mRNAs. It will be interesting to know which part of the target mRNAs RDE-12 binds. Does RDE-12 bind 5' Cap, 3' UTR, upstream of siRNA matching site or downstream of siRNA matching site? Does RDE-12 bind consensus sequence of target mRNAs? To answer these questions, CLIP (*in vivo* Cross-Linking and Immuno-Precipitation) would be the ideal approach. This method is designed for identifying protein-RNA direct interaction sites in living cell (Ule *et al.* 2005). In this approach, proteins and RNAs with direct interaction are cross-linked by UV irradiation. Most regions of RNAs, except those bound by proteins, will be degraded after RNase treatment. Those protected small pieces of RNAs will be reverse transcribed to cDNAs. Then cDNAs will be directly sequenced with the Next Generation Sequencing technology.

To identify RDE-12 interacting proteins, we could perform large scale immuno-precipitations followed by MudPIT proteomics approach. We have successfully identified RDE-11 and RDE-12 as members of the RDE-10 complex, so we expect that this experiment will identify novel components residing in RDE-12 associated foci. The helicase core can be divided into two sub-domains: domain 1 and domain 2. Recent study showed that domain 1 acts as an ATP-binding domain and domain 2 acts as an RNA binding domain (Mallam *et al.* 2012). By introducing mutation into different motifs in two domains, we will be able to disrupt the function of one domain but not the other. We will also be able to disrupt the helicase activity only but not the ATP-binding and RNA-binding activity. Our goal is to define the molecular determinants in the RDE-12 protein that are necessary for RNAi, and establish a link between RDE-12 localization and function.

mRNAs targeted by RNAi are considered to be sorted into P bodies (Liu *et al.* 2005; Eulalio *et al.* 2007). In this work, we showed RDE-12 binds target mRNAs and forms a distinct cytoplasmic foci other than P bodies. This intriguing finding suggests that target mRNAs may not be sorted into P bodies for degradation immediately in *C. elegans*. This makes intuitive sense, as target mRNAs are the templates of secondary siRNA synthesis. It will not be beneficial for the amplification of RNAi response that target mRNAs are degraded immediately. This is further supported by the siRNA deep sequencing that *rde-12(-)* mutants are defective in secondary siRNA biogenesis. mRNAs that recognized by RISC are believed to either undergoing immediate degradation or progressive depolyadenylation, which can be called the "on-site" model. The findings in this work could suggest a "drop off" model in *C. elegans*: once recognized by an Argonaute-containing complex, target mRNAs are labeled and then dropped off at a subcellular compartment where RDE-10/RDE-11 dependent degradation takes place. The "label" could be RDE-12! Identifying physical interaction between RDE-12 and Argonaute proteins will further support this idea. RDE-12 could act as the link between mRNAs targeting and secondary siRNA amplification in RNAi pathway in *C. elegans*.

It is becoming more and more apparent that the fundamental mechanism underlying various small RNA pathways is essential for our understanding of the gene expression regulation and genome stability in disease pathogenesis and essentially animal development. Since RNA mediated gene silencing shows great potential in gene therapy, the basic mechanisms of RNAi have been adapted to apply in clinical treatment. As regulatory small RNA pathways are intertwined, it is extremely important to discover what the difference among small RNA pathways is, so that we can employ one without hampering others. The work described here studied the fundamental mechanisms of RNAi pathway in nematode *C. elegans*. Considering the

similarity among small RNA pathways in different organism, these findings will provide insights on understanding small regulatory RNA pathways outside of nematode *Caenorhabditis elegans*.

Bibliography

Altschul, S. F., J. C. Wootton, et al. (2005). "Protein database searches using compositionally adjusted substitution matrices." FEBS J **272**(20): 5101-5109.

Aoki, K., H. Moriguchi, et al. (2007). "In vitro analyses of the production and activity of secondary small interfering RNAs in C. elegans." EMBO J **26**(24): 5007-5019.

Balagopal, V. and R. Parker (2009). "Polysomes, P bodies and stress granules: states and fates of eukaryotic mRNAs." Curr Opin Cell Biol **21**(3): 403-408.

Batista, P. J., J. G. Ruby, et al. (2008). "PRG-1 and 21U-RNAs interact to form the piRNA complex required for fertility in C. elegans." Mol Cell **31**(1): 67-78.

Bernstein, E., A. A. Caudy, et al. (2001). "Role for a bidentate ribonuclease in the initiation step of RNA interference." Nature **409**(6818): 363-366.

Boland, A., E. Huntzinger, et al. (2011). "Crystal structure of the MID-PIWI lobe of a eukaryotic Argonaute protein." Proc Natl Acad Sci U S A **108**(26): 10466-10471.

Buckley, B. A., K. B. Burkhart, et al. (2012). "A nuclear Argonaute promotes multigenerational epigenetic inheritance and germline immortality." Nature **489**(7416): 447-451.

Catalanotto, C., G. Azzalin, et al. (2002). "Involvement of small RNAs and role of the qde genes in the gene silencing pathway in Neurospora." Genes Dev **16**(7): 790-795.

Caudy, A. A., R. F. Ketting, et al. (2003). "A micrococcal nuclease homologue in RNAi effector complexes." Nature **425**(6956): 411-414.

Chapman, E. J. and J. C. Carrington (2007). "Specialization and evolution of endogenous small RNA pathways." Nat Rev Genet **8**(11): 884-896.

Claycomb, J. M., P. J. Batista, et al. (2009). "The Argonaute CSR-1 and its 22G-RNA cofactors are required for holocentric chromosome segregation." Cell **139**(1): 123-134.

Cogoni, C. and G. Macino (1997). "Isolation of quelling-defective (qde) mutants impaired in posttranscriptional transgene-induced gene silencing in Neurospora crassa." Proc Natl Acad Sci U S A **94**(19): 10233-10238.

Conine, C. C., P. J. Batista, et al. (2010). "Argonautes ALG-3 and ALG-4 are required for spermatogenesis-specific 26G-RNAs and thermotolerant sperm in Caenorhabditis elegans." Proc Natl Acad Sci U S A **107**(8): 3588-3593.

Ding, S. W. (2010). "RNA-based antiviral immunity." Nat Rev Immunol **10**(9): 632-644.

Duchaine, T. F., J. A. Wohlschlegel, et al. (2006). "Functional proteomics reveals the biochemical niche of C. elegans DCR-1 in multiple small-RNA-mediated pathways." Cell **124**(2): 343-354.

Elbashir, S. M., W. Lendeckel, et al. (2001). "RNA interference is mediated by 21- and 22-nucleotide RNAs." Genes Dev **15**(2): 188-200.

Eng, J., A. L. McCormack, et al. (1994). "An approach to correlate tandem mass spectral data of peptides with amino acid sequences in a protein database." J. Amer. Mass Spectrom. **5**: 976-989.

Eulalio, A., I. Behm-Ansmant, et al. (2007). "P-body formation is a consequence, not the cause, of RNA-mediated gene silencing." Mol Cell Biol **27**(11): 3970-3981.

Fire, A., D. Albertson, et al. (1991). "Production of antisense RNA leads to effective and specific inhibition of gene expression in C. elegans muscle." Development **113**(2): 503-514.

Fire, A., S. Xu, et al. (1998). "Potent and specific genetic interference by double-stranded RNA in Caenorhabditis elegans." Nature **391**(6669): 806-811.

Fischer, S. E., M. D. Butler, et al. (2008). "Trans-splicing in C. elegans generates the negative RNAi regulator ERI-6/7." Nature **455**(7212): 491-496.

Florens, L. and M. P. Washburn (2006). "Proteomic analysis by multidimensional protein identification technology." Methods Mol Biol **328**: 159-175.

Garcia, D., S. Garcia, et al. (2012). "Ago hook and RNA helicase motifs underpin dual roles for SDE3 in antiviral defense and silencing of nonconserved intergenic regions." Mol Cell **48**(1): 109-120.

Gent, J. I., A. T. Lamm, et al. (2010). "Distinct phases of siRNA synthesis in an endogenous RNAi pathway in C. elegans soma." Mol Cell **37**(5): 679-689.
Gent, J. I., M. Schvarzstein, et al. (2009). "A Caenorhabditis elegans RNA-directed RNA polymerase in sperm development and endogenous RNA interference." Genetics **183**(4): 1297-1314.
Ghildiyal, M. and P. D. Zamore (2009). "Small silencing RNAs: an expanding universe." Nat Rev Genet **10**(2): 94-108.
Grimm, D., K. L. Streetz, et al. (2006). "Fatality in mice due to oversaturation of cellular microRNA/short hairpin RNA pathways." Nature **441**(7092): 537-541.
Grishok, A., A. E. Pasquinelli, et al. (2001). "Genes and mechanisms related to RNA interference regulate expression of the small temporal RNAs that control C. elegans developmental timing." Cell **106**(1): 23-34.
Grishok, A., J. L. Sinskey, et al. (2005). "Transcriptional silencing of a transgene by RNAi in the soma of C. elegans." Genes Dev **19**(6): 683-696.
Gu, W., H. C. Lee, et al. (2012). "CapSeq and CIP-TAP identify Pol II start sites and reveal capped small RNAs as C. elegans piRNA precursors." Cell **151**(7): 1488-1500.
Gu, W., M. Shirayama, et al. (2009). "Distinct argonaute-mediated 22G-RNA pathways direct genome surveillance in the C. elegans germline." Mol Cell **36**(2): 231-244.
Guang, S., A. F. Bochner, et al. (2010). "Small regulatory RNAs inhibit RNA polymerase II during the elongation phase of transcription." Nature **465**(7301): 1097-1101.
Guang, S., A. F. Bochner, et al. (2008). "An Argonaute transports siRNAs from the cytoplasm to the nucleus." Science **321**(5888): 537-541.
Guo, S. and K. J. Kemphues (1995). "par-1, a gene required for establishing polarity in C. elegans embryos, encodes a putative Ser/Thr kinase that is asymmetrically distributed." Cell **81**(4): 611-620.
Hammond, S. M., E. Bernstein, et al. (2000). "An RNA-directed nuclease mediates post-transcriptional gene silencing in Drosophila cells." Nature **404**(6775): 293-296.
Hammond, S. M., S. Boettcher, et al. (2001). "Argonaute2, a link between genetic and biochemical analyses of RNAi." Science **293**(5532): 1146-1150.
Han, T., A. P. Manoharan, et al. (2009). "26G endo-siRNAs regulate spermatogenic and zygotic gene expression in Caenorhabditis elegans." Proc Natl Acad Sci U S A **106**(44): 18674-18679.
Iwasaki, S., M. Kobayashi, et al. (2010). "Hsc70/Hsp90 chaperone machinery mediates ATP-dependent RISC loading of small RNA duplexes." Mol Cell **39**(2): 292-299.
Izant, J. G. and H. Weintraub (1984). "Inhibition of thymidine kinase gene expression by anti-sense RNA: a molecular approach to genetic analysis." Cell **36**(4): 1007-1015.
Jankowsky, E. and M. E. Fairman (2007). "RNA helicases--one fold for many functions." Curr Opin Struct Biol **17**(3): 316-324.
Kelly, W. G., S. Xu, et al. (1997). "Distinct requirements for somatic and germline expression of a generally expressed Caernorhabditis elegans gene." Genetics **146**(1): 227-238.
Ketting, R. F., S. E. Fischer, et al. (2001). "Dicer functions in RNA interference and in synthesis of small RNA involved in developmental timing in C. elegans." Genes Dev **15**(20): 2654-2659.
Khvorova, A., A. Reynolds, et al. (2003). "Functional siRNAs and miRNAs exhibit strand bias." Cell **115**(2): 209-216.
Kim, J. K., H. W. Gabel, et al. (2005). "Functional genomic analysis of RNA interference in C. elegans." Science **308**(5725): 1164-1167.
Knight, S. W. and B. L. Bass (2001). "A role for the RNase III enzyme DCR-1 in RNA interference and germ line development in Caenorhabditis elegans." Science **293**(5538): 2269-2271.
Lau, N. C., L. P. Lim, et al. (2001). "An abundant class of tiny RNAs with probable regulatory roles in Caenorhabditis elegans." Science **294**(5543): 858-862.

Lee, H. C., A. P. Aalto, et al. (2010). "The DNA/RNA-dependent RNA polymerase QDE-1 generates aberrant RNA and dsRNA for RNAi in a process requiring replication protein A and a DNA helicase." PLoS Biol **8**(10).
Lee, R. C. and V. Ambros (2001). "An extensive class of small RNAs in Caenorhabditis elegans." Science **294**(5543): 862-864.
Lee, R. C., C. M. Hammell, et al. (2006). "Interacting endogenous and exogenous RNAi pathways in Caenorhabditis elegans." RNA **12**(4): 589-597.
Letunic, I., T. Doerks, et al. (2009). "SMART 6: recent updates and new developments." Nucleic Acids Res **37**(Database issue): D229-232.
Liu, J., M. A. Carmell, et al. (2004). "Argonaute2 is the catalytic engine of mammalian RNAi." Science **305**(5689): 1437-1441.
Liu, J., M. A. Valencia-Sanchez, et al. (2005). "MicroRNA-dependent localization of targeted mRNAs to mammalian P-bodies." Nat Cell Biol **7**(7): 719-723.
Liu, Q., T. A. Rand, et al. (2003). "R2D2, a bridge between the initiation and effector steps of the Drosophila RNAi pathway." Science **301**(5641): 1921-1925.
Luo, Z. and Z. Chen (2007). "Improperly terminated, unpolyadenylated mRNA of sense transgenes is targeted by RDR6-mediated RNA silencing in Arabidopsis." Plant Cell **19**(3): 943-958.
MacRae, I. J., K. Zhou, et al. (2007). "Structural determinants of RNA recognition and cleavage by Dicer." Nat Struct Mol Biol **14**(10): 934-940.
Mallam, A. L., M. Del Campo, et al. (2012). "Structural basis for RNA-duplex recognition and unwinding by the DEAD-box helicase Mss116p." Nature **490**(7418): 121-125.
Marchler-Bauer, A., S. Lu, et al. (2011). "CDD: a Conserved Domain Database for the functional annotation of proteins." Nucleic Acids Res **39**(Database issue): D225-229.
Martinez, J., A. Patkaniowska, et al. (2002). "Single-stranded antisense siRNAs guide target RNA cleavage in RNAi." Cell **110**(5): 563-574.
Meister, G., M. Landthaler, et al. (2004). "Human Argonaute2 mediates RNA cleavage targeted by miRNAs and siRNAs." Mol Cell **15**(2): 185-197.
Miyoshi, T., A. Takeuchi, et al. (2010). "A direct role for Hsp90 in pre-RISC formation in Drosophila." Nat Struct Mol Biol **17**(8): 1024-1026.
Montgomery, M. K. and A. Fire (1998). "Double-stranded RNA as a mediator in sequence-specific genetic silencing and co-suppression." Trends Genet **14**(7): 255-258.
Mourrain, P., C. Beclin, et al. (2000). "Arabidopsis SGS2 and SGS3 genes are required for posttranscriptional gene silencing and natural virus resistance." Cell **101**(5): 533-542.
Oka, T., T. Toyomura, et al. (2001). "Four subunit a isoforms of Caenorhabditis elegans vacuolar H+-ATPase. Cell-specific expression during development." J Biol Chem **276**(35): 33079-33085.
Pak, J. and A. Fire (2007). "Distinct populations of primary and secondary effectors during RNAi in C. elegans." Science **315**(5809): 241-244.
Pak, J., J. M. Maniar, et al. (2012). "Protection from feed-forward amplification in an amplified RNAi mechanism." Cell **151**(4): 885-899.
Pavelec, D. M., J. Lachowiec, et al. (2009). "Requirement for the ERI/DICER complex in endogenous RNA interference and sperm development in Caenorhabditis elegans." Genetics **183**(4): 1283-1295.
Phillips, C. M., T. A. Montgomery, et al. (2012). "MUT-16 promotes formation of perinuclear mutator foci required for RNA silencing in the C. elegans germline." Genes Dev **26**(13): 1433-1444.
Reinhart, B. J., F. J. Slack, et al. (2000). "The 21-nucleotide let-7 RNA regulates developmental timing in Caenorhabditis elegans." Nature **403**(6772): 901-906.
Ruby, J. G., C. Jan, et al. (2006). "Large-scale sequencing reveals 21U-RNAs and additional microRNAs and endogenous siRNAs in C. elegans." Cell **127**(6): 1193-1207.
Schwarz, D. S., G. Hutvagner, et al. (2003). "Asymmetry in the assembly of the RNAi enzyme complex." Cell **115**(2): 199-208.

Sen, G. L. and H. M. Blau (2005). "Argonaute 2/RISC resides in sites of mammalian mRNA decay known as cytoplasmic bodies." Nat Cell Biol **7**(6): 633-636.
Sheth, U., J. Pitt, et al. (2010). "Perinuclear P granules are the principal sites of mRNA export in adult C. elegans germ cells." Development **137**(8): 1305-1314.
Sijen, T., J. Fleenor, et al. (2001). "On the role of RNA amplification in dsRNA-triggered gene silencing." Cell **107**(4): 465-476.
Sijen, T., F. A. Steiner, et al. (2007). "Secondary siRNAs result from unprimed RNA synthesis and form a distinct class." Science **315**(5809): 244-247.
Smardon, A., J. M. Spoerke, et al. (2000). "EGO-1 is related to RNA-directed RNA polymerase and functions in germ-line development and RNA interference in C. elegans." Curr Biol **10**(4): 169-178.
Song, J. J., S. K. Smith, et al. (2004). "Crystal structure of Argonaute and its implications for RISC slicer activity." Science **305**(5689): 1434-1437.
Tabara, H., M. Sarkissian, et al. (1999). "The rde-1 gene, RNA interference, and transposon silencing in C. elegans." Cell **99**(2): 123-132.
Tabara, H., E. Yigit, et al. (2002). "The dsRNA binding protein RDE-4 interacts with RDE-1, DCR-1, and a DExH-box helicase to direct RNAi in C. elegans." Cell **109**(7): 861-871.
Tabb, D. L., W. H. McDonald, et al. (2002). "DTASelect and Contrast: tools for assembling and comparing protein identifications from shotgun proteomics." J Proteome Res **1**(1): 21-26.
Take-Uchi, M., M. Kawakami, et al. (1998). "An ion channel of the degenerin/epithelial sodium channel superfamily controls the defecation rhythm in Caenorhabditis elegans." Proc Natl Acad Sci U S A **95**(20): 11775-11780.
Tijsterman, M., R. F. Ketting, et al. (2002). "RNA helicase MUT-14-dependent gene silencing triggered in C. elegans by short antisense RNAs." Science **295**(5555): 694-697.
Tijsterman, M., R. C. May, et al. (2004). "Genes required for systemic RNA interference in Caenorhabditis elegans." Curr Biol **14**(2): 111-116.
Timmons, L., D. L. Court, et al. (2001). "Ingestion of bacterially expressed dsRNAs can produce specific and potent genetic interference in Caenorhabditis elegans." Gene **263**(1-2): 103-112.
Tomari, Y., C. Matranga, et al. (2004). "A protein sensor for siRNA asymmetry." Science **306**(5700): 1377-1380.
Ule, J., K. Jensen, et al. (2005). "CLIP: a method for identifying protein-RNA interaction sites in living cells." Methods **37**(4): 376-386.
Updike, D. and S. Strome (2010). "P granule assembly and function in Caenorhabditis elegans germ cells." J Androl **31**(1): 53-60.
Updike, D. L., S. J. Hachey, et al. (2011). "P granules extend the nuclear pore complex environment in the C. elegans germ line." J Cell Biol **192**(6): 939-948.
Vasale, J. J., W. Gu, et al. (2010). "Sequential rounds of RNA-dependent RNA transcription drive endogenous small-RNA biogenesis in the ERGO-1/Argonaute pathway." Proc Natl Acad Sci U S A **107**(8): 3582-3587.
Weinberg, D. E., K. Nakanishi, et al. (2011). "The inside-out mechanism of Dicers from budding yeasts." Cell **146**(2): 262-276.
Winston, W. M., C. Molodowitch, et al. (2002). "Systemic RNAi in C. elegans requires the putative transmembrane protein SID-1." Science **295**(5564): 2456-2459.
Wu-Scharf, D., B. Jeong, et al. (2000). "Transgene and transposon silencing in Chlamydomonas reinhardtii by a DEAH-box RNA helicase." Science **290**(5494): 1159-1162.
Yang, H., Y. Zhang, et al. (2012). "The RDE-10/RDE-11 complex triggers RNAi-induced mRNA degradation by association with target mRNA in C. elegans." Genes Dev **26**(8): 846-856.
Yigit, E., P. J. Batista, et al. (2006). "Analysis of the C. elegans Argonaute family reveals that distinct Argonautes act sequentially during RNAi." Cell **127**(4): 747-757.

Zhang, C., T. A. Montgomery, et al. (2011). "mut-16 and other mutator class genes modulate 22G and 26G siRNA pathways in Caenorhabditis elegans." Proc Natl Acad Sci U S A **108**(4): 1201-1208.
Zhang, H., F. A. Kolb, et al. (2004). "Single processing center models for human Dicer and bacterial RNase III." Cell **118**(1): 57-68.
Zhang, Y., Z. Wen, et al. (2010). "Refinements to label free proteome quantitation: how to deal with peptides shared by multiple proteins." Anal Chem **82**(6): 2272-2281.